RSC Advances

ROYAL SOCIETY OF CHEMISTRY

PAPER

View Article Online
View Journal | View Issue

Check for updates

Cite this: *RSC Adv.*, 2025, **15**, 1391

Synthesis and modification of novel thiazole-fused quinoxalines as new insecticidal agents against the cotton leafworm *Spodoptera litura*: design, characterization, *in vivo* bio-evaluation, toxicological effectiveness, and study their mode of action†

Doaa M. Elsisi,[a] Moustafa S. Abusaif,*[b] Eman El-Said,*[c] Enayat M. Elqady,[c] Mohamed A. Salem,[d] Yousry A. Ammar[b] and Ahmed Ragab *[be]

Herein, novel thiazolo[4,5-*b*]quinoxalin-2-ones **2–6** and thiazolo[4,5-*b*]quinoxalin-2(3*H*)-imines **7–9** were synthesized and characterized using elemental analysis, IR spectroscopy, and $^{1}H/^{13}C$ NMR to confirm their structures. The efficacy of the newly designed thiazolo-quinoxalines **2**, **3**, **4**, **5**, **7**, **8**, and **9** against the cotton leafworm *S. litura* (2nd and 4th instar larvae) was evaluated, and results revealed insecticidal activity with variable and good mortality percentages. A SAR study was also discussed. Additionally, compound **3** exhibited the highest insecticidal activity, with mortality% values ranging from 86% ± 7.21% to 97% ± 1.52% and from 66.00% ± 6.24% to 86.33% ± 6.90% at concentrations of 625–2500 mg L^{-1} against the 2nd and 4th instar larvae, respectively. The probit analysis revealed that the thiazolo[4,5-*b*]quinoxalin-2(3*H*)-one derivative **3**, after 5 days of treatment, exhibited LC_{50} values of 141.02 and 366.73 mg L^{-1} for the 2nd and 4th instar larvae, respectively. The LT_{50} values ranged from 0.52 to 1.92 days for the 2nd larval instar and from 1.95 to 2.47 days for the 4th larval instar. The corresponding toxicity index (TI) values were 86.21% for the 2nd instar and 78.47% for the 4th instar larvae. The mode of action of compound **3** was assessed through physiological, histological, and SEM analyses on the 4th larval instar. The physiological bioassay revealed a significant increase in total carbohydrate and protein levels compared to the control group. However, the enzymatic study showed a significant decrease ($P < 0.05$) in the levels of aspartate aminotransferase (AST/GOT), alanine aminotransferase (ALT/GPT), and alkaline phosphatase (AlP), while acetylcholinesterase (AChE) levels significantly increased. SEM analysis revealed malformations in the external body, while histological examination demonstrated severe damage to the gut epithelium and regenerative cells in the midgut tissues.

Received 14th November 2024
Accepted 25th December 2024

DOI: 10.1039/d4ra08096c

rsc.li/rsc-advances

Open Access Article. Published on 16 January 2025. Downloaded on 2/25/2025 6:25:58 AM.
This article is licensed under a Creative Commons Attribution-NonCommercial 3.0 Unported Licence.

1. Introduction

Spodoptera litura, commonly known as the tobacco cutworm or cotton leafworm, is a highly significant pest for plants.[1] This agricultural pest is distributed across various regions worldwide and has an extensive host range, affecting crops such as cotton, tobacco, soybeans, tomatoes, and corn.[2] Additionally, *S. litura* is a major destructive pest that poses a significant threat to numerous field crops and vegetables in Egypt, as well as in other countries across the Middle East and North Africa.[3] Cotton farming, a vital economic resource for Egypt, is particularly vulnerable to this pest.[4] Moreover, *S. litura* is considered one of the most harmful pests of over 60 other economically important crops, ornamentals, and vegetables.[5,6] Additionally, one of the major issues caused by *S. litura* is defoliation. The larvae of this insect feed extensively on plant leaves, leading to extensive damage to the foliage. This damage impairs photosynthesis, which in turn negatively affects plant growth and overall productivity.[7] Another significant issue associated with *S. litura* is its ability to develop resistance to insecticides. Over time, the

[a]*Department of Chemistry, Faculty of Science (Girls), Al-Azhar University, 11754 Nasr City, Cairo, Egypt*
[b]*Department of Chemistry, Faculty of Science (Boys), Al-Azhar University, 11884 Nasr City, Cairo, Egypt. E-mail: mostafahozaifa317@azhar.edu.eg; Ahmed_ragab@azhar.edu.eg*
[c]*Zoology and Entomology Department, Faculty of Science, Al-Azhar University (Girls), Cairo, Egypt. E-mail: emanGommaa1465.el@azhar.edu.eg*
[d]*Department of Chemistry, Faculty of Science and Arts, King Khalid University, Mohail, Assir, Saudi Arabia*
[e]*Chemistry Department, Faculty of Science, Galala University, Galala City, Suez, 43511, Egypt. E-mail: Ahmed.abdelwahab@Gu.edu.eg*

† Electronic supplementary information (ESI) available. See DOI: https://doi.org/10.1039/d4ra08096c

© 2025 The Author(s). Published by the Royal Society of Chemistry

Open Access Article. Published on 16 January 2025. Downloaded on 2/25/2025 6:25:58 AM. This article is licensed under a Creative Commons Attribution-NonCommercial 3.0 Unported Licence.

repeated application of certain chemical treatments can drive the evolution of resistant strains of this pest. This situation presents a significant challenge to farmers, necessitating the implementation of integrated pest management strategies to effectively control *S. litura* populations.[8] Moreover, the feeding activity of *S. litura* larvae can open up pathways for secondary infections by fungal or bacterial pathogens. These opportunistic pathogens exploit the weakened plant tissues, thereby exacerbating the damage caused by the insect.[9]

Thiazole derivatives have been extensively studied in medicinal chemistry owing to their pharmacological activities and potential therapeutic applications, such as antimicrobial, anticancer,[10,11] antimicrobial,[12,13] antidiabetics,[14] antioxidant,[15] anti-inflammatory,[16] analgesic,[17] and anticonvulsant[18] effects. These properties have expanded the potential applications of thiazole-based compounds in diverse therapeutic fields. Moreover, thiazole derivatives have gained notable importance in the fields of agrochemistry and medicine owing to their diverse range of activities and potential applications. As agrochemicals, they exhibit fungicidal[19] and herbicidal[20] activities, making them valuable tools for crop protection. Several studies have investigated the insecticidal properties of thiazole derivatives against various insect pests, including mosquitoes,[21] flies,[22] and moths.[23] These compounds have shown promising results in terms of controlling insect populations and minimizing the harm they cause to crops, livestock, and humans. Thiazole derivatives are utilized in numerous insecticides, such as thiamethoxam (**I**), which effectively combats a range of agricultural pests, including aphids, leafhoppers, whiteflies, and beetles.[24] Another example is thiacloprid (**II**), which is used to control chewing and sucking insect pests in a wide range of crops, including fruits, vegetables, and ornamental plants[25] (Fig. 1).

Furthermore, quinoxalines are versatile heterocyclic compounds that have garnered considerable interest in the fields of medicinal and agrochemistry. This is primarily due to their wide range of biological activities, including antimicrobial,[26] anti-inflammatory,[27] anticancer,[28,29] antioxidant,[30] antidiabetic,[31] antiviral,[32] and insecticidal[33] properties. Among these compounds, chlorquinox (**III**) is a broad-spectrum insecticide belonging to the quinoxaline family. It is commonly used to control unwanted pests, such as insects, acaricides, nematodes, and phytopathogenic fungi.[34] Oxythioquinox (chinomethionat) (**IV**) was first approved for use in the United States in 1968 as a multipurpose agent against insects, mites, and fungal diseases. Moreover, both quizalofop-methyl (**V**) and quizalofop-*p*-tefuryl (**VI**) contain a quinoxaline core that serves as herbicide safeners[35–37] (Fig. 1).

Based on the aforementioned findings related to the discovery of new bioactive agents used as insecticides against *S. litura* and our experience in modifying new heterocyclic moieties to overcome the mutation and resistance of cells and microbial strains,[38–42] this study designs a new thiazole fused with a quinoxaline ring. This led to one hybrid molecule known as thiazolo[4,5-*b*]quinoxaline derivatives **2–9**, hoping to enhance insecticidal efficacy in combating *S. litura*. The designed derivatives were evaluated by calculating the mortality percentage at concentrations of 2500, 1250, and 625 mg L^{-1} after 3, 5, and 7 days of treatments, respectively, compared with lufenuron as the positive control. Toxicological effectiveness (LC_{50} and LT_{50} estimates) was also checked for the 2nd and 4th larval instars. Moreover, the mode of action of the most active derivative **3** was assessed through physiological, histological, and SEM analyses of the 4th larval stage.

2. Results and discussion

2.1. Chemistry

The synthetic routes of the thiazolo[4,5-*b*]quinoxaline derivatives are displayed in Schemes 1 and 2 using 2,3-

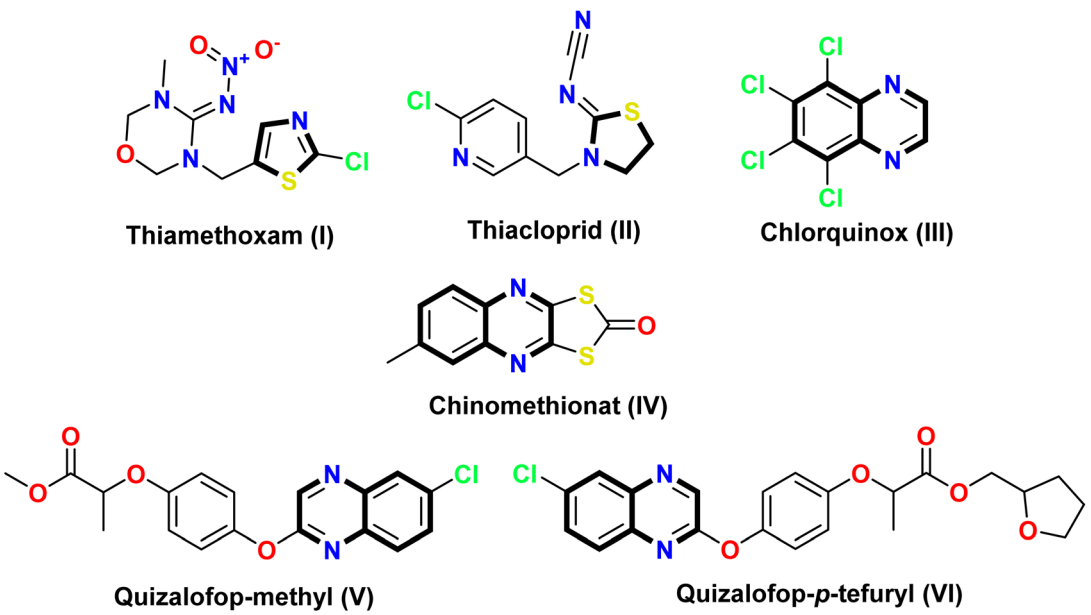

Fig. 1 Structures of some insecticidal agents containing thiazole and quinoxaline cores.

© 2025 The Author(s). Published by the Royal Society of Chemistry

Open Access Article. Published on 16 January 2025. Downloaded on 2/25/2025 6:25:58 AM.
This article is licensed under a Creative Commons Attribution-NonCommercial 3.0 Unported Licence.

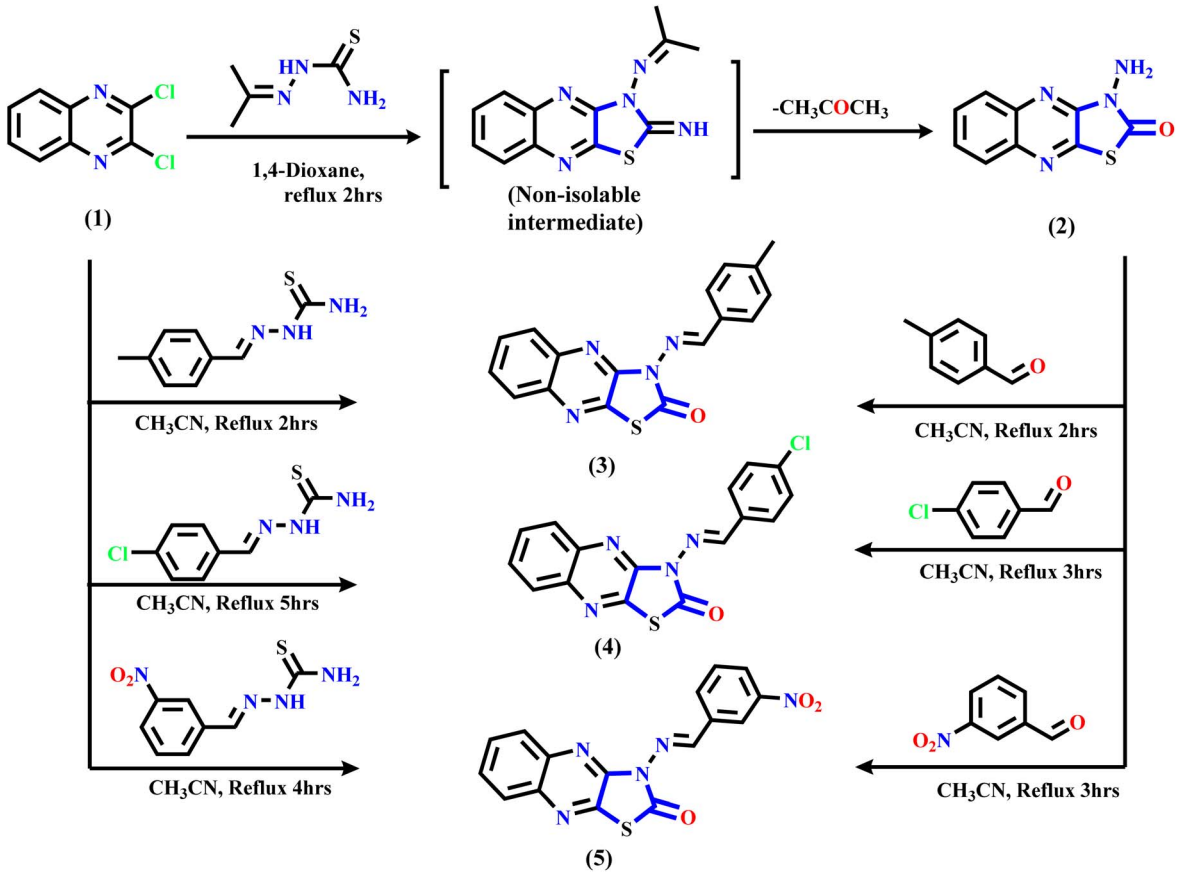

Scheme 1 Illustration of the synthesis of bioactive thiazolo[4,5-*b*]quinoxalin-2(3*H*)-one derivatives **2–5**.

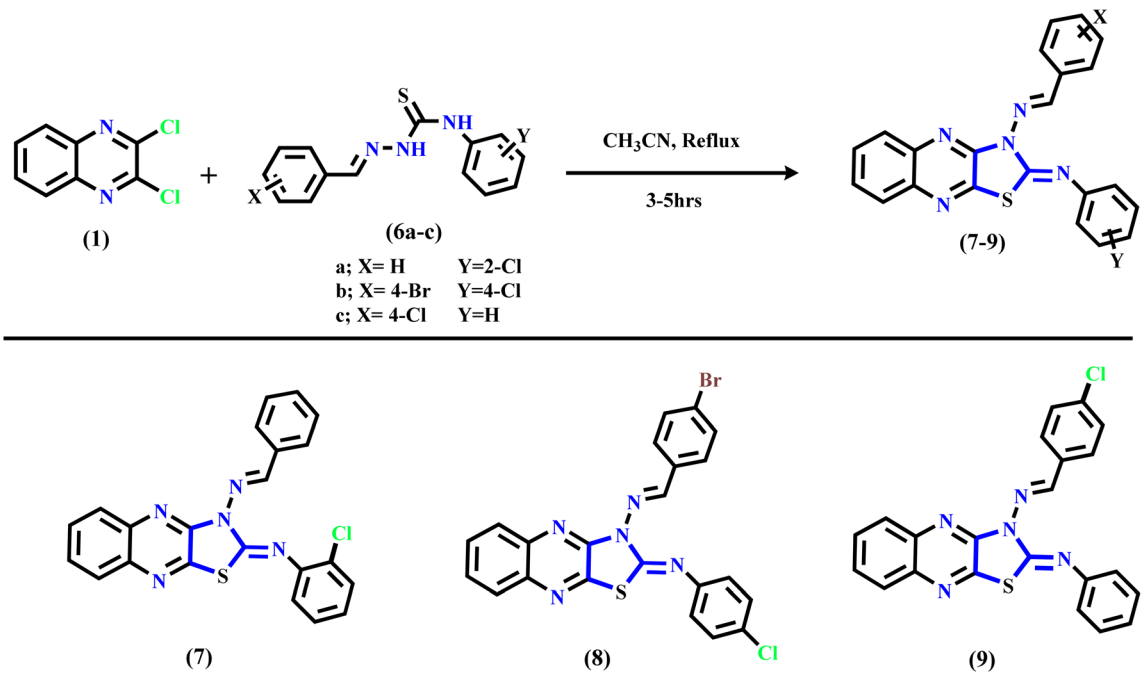

Scheme 2 Illustration of the synthesis of bioactive thiazolo-quinoxaline compounds **7–9**.

Open Access Article. Published on 16 January 2025. Downloaded on 2/25/2025 6:25:58 AM. This article is licensed under a Creative Commons Attribution-NonCommercial 3.0 Unported Licence.

dichloroquinoxaline **1** (ref. 43 and 44) as a starting material, which contains two electrophilic active centers (2C–Cl functions) that can react with bi-nucleophile reagents through nucleophilic substitution reactions. As shown in Scheme 1, starting material **1** was allowed to react with acetone thiosemicarbazone, such as a bi-nucleophile reagent, to yield non-isolable intermediate 3-(propan-2-ylideneamino)thiazolo[4,5-*b*]quinoxalin-2(3*H*)-imine, followed by the elimination of the acetone molecule as the leaving group; then, the imine function (C=NH) was hydrolyzed under the reaction conditions to afford the final product 3-aminothiazolo[4,5-*b*]quinoxalin-2(3*H*)-one **2**. The structure was approved using spectral and analytical data. The IR spectrum of compound **2** showed two characteristic absorption bands for amino and carbonyl functions at ν 3246, 3133, and 1659 cm^{-1}. The ^1H NMR spectral data showed sharp singlet signals at δ 7.32 ppm assignable to the *N*-amino proton function besides the quinoxaline aromatic protons, which appeared as two triplet signals at δ 7.61 and 7.70 ppm with the coupling constant (H, $J = 8.0$ Hz) equivalent to two protons, and one doublet signal at δ 7.89 ppm with the coupling constant (H, $J = 8.0$ Hz) equivalent to two protons. Besides, the ^{13}C NMR spectral revealed specific signals in the downfield region at δ 140.01, 144.59, and 155.15 ppm corresponding to two C=N and carbonyl functions. Besides, signals are in the range of δ 125.42–137.05 ppm due to six aromatic carbons.

Furthermore, Scheme 1 displays the chemical structure of the target three active compounds **3**, **4**, and **5**, which can be prepared and confirmed chemically using two different methods. The first method involved the reaction of starting material **1** with thiosemicarbazone derivatives, namely, 2-(4-methylbenzylidene)hydrazine-1-carbothioamide, 2-(4-chlorobenzylidene)hydrazine-1-carbothioamide, and 2-(3-nitrobenzylidene)hydrazine-1-carbothioamide respectively, refluxed in acetonitrile as a solvent. The second method involved the reaction 3-aminothiazolo[4,5-*b*]quinoxalin-2(3*H*)-one **2** *via* *N*-amino function with different aromatic aldehydes specified, *p*-tolualdehyde, 4-chlorobenzaldehyde, and 3-nitrobenzaldehyde, respectively, which were heated under reflux in the presence of acetonitrile (CH_3CN) as a solvent. In addition, the chemical structure of the target three bioactive 3-aminothiazolo[4,5-*b*]quinoxalin-2(3*H*)-one derivatives **3–5** was confirmed based on analytical and spectral data.

For example, the IR spectrum of compound **3** showed three absorption bands for sp^3-CH, carbonyl, and CH=N at ν 2972, 1654, and 1602 ppm, respectively. The ^1H NMR spectral of the same compound confirmed the presence of methyl protons as a singlet signal at δ 2.06 ppm, a singlet signal in the down-field region at δ 8.45 ppm related to methylinic-H protons, and the aromatic protons appearing as two triplet and three doublet signals with a mean coupling constant ($J = 7.2$ Hz) ranging from δ 7.47 to 7.68 ppm. The ^{13}C NMR spectral exhibited specific signals at δ 22.08, 136.67, 151.86, and 162.32 ppm related to methyl carbon, CH=N, C=N, and C=O functions, respectively, in addition to ten aromatic carbon signals ranging from δ 120.42 ppm to 136.23 ppm corresponding to fourteen carbons.

Subsequently, refluxing 2,3-dichloroquinoxaline **1** in acetonitrile solution with substituted thiosemicarbazone derivatives **6a–c** afforded the corresponding *N*-(substituted-phenyl)thiazolo[4,5-*b*]quinoxalin-2(3*H*)-imine derivatives **7–9** through nucleophilic addition of the mercapto group into the C–Cl at C2 of 2,3-dichloro-quinoxaline **1**, followed by intramolecular cyclization *via* hydrogen chloride elimination by the second nucleophilic addition of the NH function into another C–Cl at C3 position in compound **1** to yield the final products **7–9** (see Scheme 2). The suggested mechanism is illustrated in the ESI (Scheme SI†). The IR spectrum of quinoxaline derivative **7** displayed two characteristic absorption bands at ν 3061, 3035, and 1620 cm^{-1}, related to sp^2-C and C=N functions, respectively. Similarly, the ^1H NMR displayed only a singlet signal for methylinic-H at δ 8.27 ppm besides the aromatic protons at δ 7.14–7.96 ppm assignable to fourteen protons. Additionally, the ^{13}C NMR of the same compounds revealed significant signals at δ 147.93 and 154.36 ppm due to the two C=N groups, respectively, besides the aromatic carbons ranging from δ 120.24 to 139.59 ppm, which were equivalent to twenty aromatic carbons.

Finally, compound **9** was isolated as a deep-red powder with a melting point (M. p.) of 277–279 °C with an acceptable yield. The ^1H NMR exhibited new methylinic-H as a singlet signal at δ 8.46 ppm and the aromatic protons in the range of δ 7.00–7.78 ppm. Moreover, its ^{13}C NMR spectrum showed two singlet signals in the down-field region at δ 144.15 and 153.95 ppm assigned to C=N and C=N functions, and aromatic carbons related to 20 carbons appeared from δ 119.43 ppm to 141.11 ppm.

2.2. Insecticidal activity

2.2.1. *In vivo* insecticidal efficiency screening derivatives on 2nd and 4th larval instars of cotton leafworm *S. litura*. The insecticidal screening of the designed thiazolo[4,5-*b*]quinoxalin-2-one **2–6** and thiazolo[4,5-*b*]quinoxalin-2(3*H*)-imine **7–9** against the most feeding stages of *S. litura* (2nd and 4th larvae) was evaluated by calculating the mortality percentage at conc. 2500, 1250, and 625 mg L^{-1} after 3, 5, and 7 days of treatments, respectively, (Table 1) compared with the recommended insecticide (lufenuron). The results revealed that all the tested thiazolo[4,5-*b*]quinoxaline derivatives **2**, **3**, **4**, **5**, **7**, **8**, and **9** have insecticidal activity with variable and good mortality percentages. Statistical analysis indicated a significant difference between treatments based on the analysis of variance (ANOVA). Tukey's Honest Significant Difference (HSD) test at $p \leq 0.05$ was performed on 42 treatments of the designed quinoxaline derivatives against *S. litura* 2nd and 4th instar larvae. Generally, the mortality percentage exhibited higher values on the 2nd larval instars compared to the 4th larval instars at the same concentration.

For the second larval instars of *S. litura*, the 3-((4-methylbenzylidene)amino) thiazolo[4,5-*b*]quinoxalin-2(3*H*)-one (**3**) exhibited the most active member with the highest mortality percentage values in the range of 86 ± 7.21–97 ± 1.52% over concentrations ranging from 625 to 2500 mg L^{-1}. Moreover, for the other 2-oxo-thiazolo[4,5-*b*]quinoxaline derivatives **2**, **4**, and **5**, a slight difference was observed in the mortality percentage, which was attributed to the different substituents on the 3-

© 2025 The Author(s). Published by the Royal Society of Chemistry

Open Access Article. Published on 16 January 2025. Downloaded on 2/25/2025 6:25:58 AM. This article is licensed under a Creative Commons Attribution-NonCommercial 3.0 Unported Licence.

Table 1 Corrected mortality% of 2nd and 4th larval instars of *S. litura* treated with the designed quinoxaline derivatives **2–5** and **7–9**[a]

	Total mean mortality%* on 3, 5, and 7 days ± S. E.					
	2nd larval instar			4th larval instar		
Cpd. no.	2500	1250	625	2500	1250	625
2	73.33 ± 13.01	63.00 ± 13.05	48.33 ± 10.7	50.00 ± 7.50	32.33 ± 6.33	24.00 ± 4.72
3	97.00 ± 1.52	95.00 ± 2.51	86.00 ± 7.21	86.33 ± 6.90	76.67 ± 6.89	66.00 ± 6.24
4	75.67 ± 10.68	63.33 ± 7.12	49.33 ± 5.60	59.33 ± 12.44	42.67 ± 9.06	27.67 ± 9.02
5	76.67 ± 8.11	62.67 ± 8.11	50.33 ± 12.09	65.67 ± 10.98	50.33 ± 12.44	37.33 ± 14.09
7	74.33 ± 8.51	64.33 ± 12.38	48.33 ± 7.53	70.33 ± 2.90	53.66 ± 3.84	37.00 ± 5.29
8	94.33 ± 2.02	67.33 ± 3.17	46.00 ± 5.29	78.33 ± 4.09	53.00 ± 3.21	32.33 ± 6.17
9	69.66 ± 12.25	59.66 ± 8.29	42.66 ± 4.80	56.33 ± 4.05	44.66 ± 4.05	35.00 ± 4.72
*P. C.	98.00 ± 1.73	96.33 ± 3.21	90.00 ± 8.67	94.00 ± 4.58	88.33 ± 7.26	80.00 ± 10.41
Control	0.00 ± 0.00	0.00 ± 0.00	0.00 ± 0.00	0.00 ± 0.00	0.00 ± 0.00	0.00 ± 0.00
$F_{df(23,48)}$ value	4.98***				7.23***	
P-Value	<0.001				<0.001	
L. S. R. ± SE	44.27 ± 11.49				41.51 ± 10.78	

[a] $F_{df(47,95)} = 6.94$*** and $p < 0.001$; *P. C. = positive control (lufenuron) df (degrees of freedom). Tukey HSD test as post Hoc. L. S. R. least significant range.

(benzylidene)amino group with different electronic characteristics. The mortality percentage of 2-oxo-thiazolo[4,5-*b*]quinoxaline derivatives **2**, **4**, and **5** demonstrated values ranging from (73.33 ± 13.01 to 76.67 ± 8.11), (62.67 ± 8.11 to 63.33 ± 7.12), and (48.33 ± 10.7 to 50.33 ± 12.09%), at concentrations of 2500, 1250, and 625 mg L^{-1}, respectively, indicating that the hydrophobic moiety at the azomethine group is important in the activity. Additionally, the 2,3-disubstituted-thiazolo[4,5-*b*] quinoxaline derivatives **7–9** displayed good to moderate mortality values. Moreover, introducing the two halogenated atoms in the two hydrophobic benzene rings at positions two and three in the thiazole nucleus, as shown in compound **8**, causes an increase in the mortality percentage to 94.33 ± 2.02, 67.33 ± 3.17, and 46.00 ± 5.29% for concentrations of 2500, 1250, and 625 mg L^{-1}, respectively.

For the old instars (4th larval), it was found that higher mortality was observed with high progressive doses. In addition, the highest mortality percentage was observed with 2-oxo-thiazolo[4,5-*b*]quinoxaline derivative **3**, followed by thiazolo [4,5-*b*]quinoxaline derivative **8** with mortality percentage values of (86.33 ± 6.90, 76.33 ± 6.89, and 66.00 ± 6.24%) and (78.33 ± 4.09, 53.00 ± 3.21, and 32.33 ± 6.17%) at concentrations of 2500, 1250, and 625 mg L^{-1}, respectively. Additionally, the minimum mortality percentage was exhibited by thiazolo[4,5-*b*] quinoxaline derivative **9** with mortality percentages of 56.33 ± 4.05, 44.66 ± 4.05, and 35.00 ± 4.72% at concentrations of 2500, 1250, and 625 mg L^{-1}, respectively, with nearly 1.23-, 1.33- and 1.21-fold higher activity than the corresponding second larval at the same concentrations.

2.2.2. Toxicological effectiveness against *S. litura* larvae with structural–activity relationship studies. A toxicological evaluation for the designed quinoxaline derivatives **2–5** and **7–9** after treatment with *S. litura* larvae in the 2nd and 4th instars was performed after five days. The represented data in Tables 2,

Table 2 Lethal concentration (LC_{50}) and lethal time (LT_{50}) of newly tested thiazolo[4,5-*b*]quinoxaline derivatives on 2nd instar larvae of *S. litura*[a]

		95% of confidence limit for conc. Mg L^{-1}						95% confidence limits for days LT_{50} (upper–lower)		
Cpd. no.	LC_{50}	Lower	Upper	Slope ± S. E.	X^2 (Sig.)	TI	R^2 (R. E.)	625	1250	2500
2	798.78	480.42	1048.51	1.28 ± 0.31	0.50 (0.48)	15.23	0.974 ($\hat{y} = -4.06 + 1.42x$)	4.92 (4.28–5.71)	3.61 nil	3.09 (2.63–3.46)
3	141.02	6.67	309.24	1.46 ± 0.45	0.38 (0.54)	86.21	86.21 ($\hat{y} = -3.06 + 143x$)	1.92 (nil)	0.73 (nil)	0.52 (nil)
4	740.44	427.28	751.38	1.29 ± 0.31	0.16 (0.69)	16.42	0.992 ($\hat{y} = -4.06 + 1.43x$)	4.87 (3.38–7.57)	2.91 (1.45–3.69)	2.76 (2.14–3.19)
5	505.85	145.04	763.11	1.06 ± 0.31	0.32 (0.57)	24.03	0.975 ($\hat{y} = -2.6 + 1x$)	4.73 (4.91–5.34)	3.22 (2.15–3.88)	2.33 (1.41–2.92)
7	820.13	342.85	1167.61	0.94 ± 0.30	0.50 (0.48)	14.82	0.953 ($\hat{y} = -2.41 + 0.86x$)	4.99 (4.07–6.41)	3.38 (nil)	2.37 (nil)
8	754.59	617.52	875.09	2.68 ± 0.36	2.24 (0.13)	16.11	0.970 ($\hat{y} = -7.14 + 2.57x$)	5.74 (4.32–14.48)	1.31 (nil)	0.49 (0.00–1.43)
9	1148.52	682.21	1735.13	0.93 ± 0.29	0.42 (0.52)	10.58	0.950 ($\hat{y} = -2.61 + 0.86x$)	7.07 (5.15–231.76)	3.42 (nil)	3.05 (nil)
P. C.	121.75	3.08	285.58	1.51 ± 0.49	0.52 (0.47)	100	0.939 ($\hat{y} = -2.86 + 1.43x$)	1.14 (nil)	0.57 (nil)	0.23 (nil)

[a] X^2 = (Sig. significance level) chi square Pearson goodness-of-fit test for probit linear analysis at $p \leq 0.05$. TI = toxicity index compared with positive control on 2nd larval instar of *S. litura*. R^2 = regression coefficients (regression equation (R. E.) $\hat{y} = a + \beta x$) for tested compounds. P. C. = positive control (lufenuron).

Open Access Article. Published on 16 January 2025. Downloaded on 2/25/2025 6:25:58 AM. This article is licensed under a Creative Commons Attribution-NonCommercial 3.0 Unported Licence.

Table 3 Lethal concentration (LC_{50}) and lethal time (LT_{50}) of newly tested thiazolo[4,5-*b*]quinoxaline derivatives on 4th instar larvae of *S. litura*[a]

Cpd. no.	LC_{50}	95% of confidence limits for conc. Mg L^{-1}		Slope ± S. E.	X^2 (Sig.)	TI	R^2 (R. E.)	95% confidence limits for days LT_{50} (lower–upper)		
		Lower	Upper					625	1250	2500
2	2562.72	1783.53	6892.92	1.07 ± 0.31	0.054 (0.82)	11.23	0.996 ($\hat{y} = -3.4 + 1x$)	14.59 (8.90–261.45)	9.01 (6.78–23.62)	4.72 (3.78–5.88)
3	366.73	108.15	573.09	1.29 ± 0.33	0.48 (0.49)	78.47	0.972 ($\hat{y} = 3.66 + 1.43x$)	2.47 (0.73–3.35)	1.96 (0.75–2.71)	1.95 (1.16–2.49)
4	1333.59	1071.78	1691.24	1.60 ± 0.31	0.003 (0.96)	21.58	0.998 ($\hat{y} = -5.23 + 1.71x$)	8.08 (6.78–11.44)	5.79 (4.97–7.39)	3.89 (3.33–4.36)
5	820.05	341.02	1168.48	0.94 ± 0.30	0.08 (0.77)	35.09	0.992 ($\hat{y} = -2.9 + 1x$)	5.94 (5.42–6.71)	4.71 (4.17–5.29)	3.32 (2.66–3.80)
7	1123.89	871.50	1401.86	1.56 ± 0.31	0.05 (0.83)	25.60	0.998 ($\hat{y} = -4.26 + 1.42x$)	8.72 (6.25–67.00)	3.68 (nil)	0.97 (nil)
8	1136.75	948.65	1341.89	2.09 ± 0.31	0.13 (0.72)	25.31	0.997 ($\hat{y} = -6.0 + 2x$)	9.42 (6.89–31.84)	3.71 (nil)	1.09 (0.001–2.17)
9	1705.56	1233.04	3167.24	1.02 ± 0.30	0.02 (0.90)	16.87	0.999 ($\hat{y} = -3.2 + 1x$)	10.38 (6.82–1030.67)	6.56 (nil)	3.21 (0.00–4.53)
*P. C.	287.76	108.39	434.98	2.09 ± 0.47	0.006 (0.99)	100	0.998 ($\hat{y} = -4.8 + 2x$)	2.50 (nil)	2.13 (nil)	1.83 (0.99–2.31)

[a] X^2 (Sig.) = chi square Pearson goodness-of-fit test at $p \leq 0.05$. TI = toxicity index compared with positive control on 4th larval instar of *S. litura*. R^2 = regression coefficients (regression equation (R. E.) $\hat{y} = a + bx$) for tested compounds. *P. C. = positive control (lufenuron).

3 and Fig. SI1,† 2 show the lethal concentration (LC_{50}), toxicity index, slope, coefficients and equations of regression of the tested compounds on 2nd and 4th larval instar of *S. litura* for 5 days of treatment. The simple linear regression showed that the regression coefficients R^2 were very close to 1, indicating that residual values were very small between the expected and observed responses in the probit analysis. Additionally, the regression equation showed a positive correlation between concentrations x and mortality% y for 2nd and 4th *S. litura* larvae.

2.2.2.1. Toxicological effectiveness (LC_{50} and LT_{50} estimates) checking for 2nd larval instar. The probit analysis for the synthesized thiazolo[4,5-*b*]quinoxaline derivatives indicated that 3-((4-methyl benzylidene)amino)thiazolo[4,5-*b*]quinoxalin-2(3*H*)-one (**3**) was the most effective compound with LC_{50} = 141.02 mg L^{-1}, followed by quinoxaline derivatives **5**, **4**, **8**, **2**, and **7** with the LC_{50} values of 505.85, 740.44, 754.59, 798.78, 820.13 and 1148.52 mg L^{-1}, respectively. Moreover, the slope values revealed that 2,3-disubstituted thiazolo[4,5-*b*]quinoxalin-2(3*H*)-imine derivative **8** had the highest value of 1.06 ± 0.31, while the other quinoxaline derivatives **3**, **4**, **2**, **5**, **7** and **9** compounds had slope values of 1.46 ± 0.45, 1.29 ± 0.31, 1.28 ± 0.31, 1.06 ± 0.31, 0.94 ± 0.30, and 0.93 ± 0.29, respectively. Additionally, the data revealed that 2-oxo-thiazolo[4,5-*b*]quinoxaline derivative **3** demonstrated the toxicity index (TI) at LC_{50} = 141.02 mg L^{-1}, which was 86.21%, while the other derivatives recorded 24.03%, 16.42%, 16.11%, 15.23%, 14.82% and 10.58% for quinoxaline derivatives **5**, **4**, **8**, **2**, **7** and **9**, respectively, compared to recommended insecticide (lufenuron) (Table 2).

According to the lethal time (LT_{50}) values of the tested thiazolo[4,5-*b*]quinoxaline derivatives **2–5** and **7–9**, it was found that compound **3** had the lowest time with 0.52, 0.73, and 1.92 days overall concentrations (2500, 1250, and 625 mg L^{-1}, respectively), compared to lufenuron. Additionally, comparing the structures of quinoxaline derivatives **4** and **8**, we found that replacing the carbonyl group at C2 of 2-oxo-thiazolo[4,5-*b*]quinoxaline derivative **3** with *N*-(4-bromophenyl) caused a slight decrease in the toxicological activity of nearly 14.15 mg L^{-1}, indicating that the hydrophobic moiety with (4-bromophenyl) did not enhance insecticidal activity. In the same way, replacing the position of chlorine with the *meta* position and replacing the two aryl groups, as shown in quinoxaline derivatives **7** (LC_{50} = 820.13 mg L^{-1}) and **9** (LC_{50} = 1148.52 mg L^{-1}), revealed that the presence of chlorine in the *para* position at *N*-(4-chlorophenyl)thiazolo[4,5-*b*]quinoxaline **9** enhanced insecticidal activity.

However, the highest lethal time (LT_{50}) values were introduced by 2,3-disubstituted thiazolo[4,5-*b*]quinoxalin-2(3*H*)-imine derivatives **7**, **8**, and **9** at low concentrations (625 mg L^{-1}) with LT_{50} values of 4.99, 5.74, and 7.07 days, respectively, followed by 2-oxo-thiazolo[4,5-*b*]quinoxalines **2–5**. Surprisingly, the 2,3-(halogenated aryl)thiazolo[4,5-*b*]quinoxalin-2(3*H*)-imine derivatives **8** demonstrated the lowest LT_{50} = 0.49 day, indicating that the activity may be due to the chlorine and bromine atoms at the two aryl groups attached at C2 and C3 of thiazolo[4,5-*b*]quinoxalin-2(3*H*)-imine derivative **8**. In addition, at a high concentration (2500 mg L^{-1}), the order of lethal time changed to **8** (0.49) > **3** (0.52) > **5** (2.33) > **7** (2.37) > **4** (2.76) > **9** (3.05) > **2** (3.09) (Table 2). Previous results proved that all tested quinoxaline derivatives exhibited good toxicity effects and compound **3** was the most effective, whereas quinoxaline derivative **9** was the least effective.

© 2025 The Author(s). Published by the Royal Society of Chemistry

Open Access Article. Published on 16 January 2025. Downloaded on 2/25/2025 6:25:58 AM. This article is licensed under a Creative Commons Attribution-NonCommercial 3.0 Unported Licence.

2.2.2.2. Toxicological effectiveness (LC_{50} and LT_{50} estimates) checking for 4th larval instar. In general, as described in Table 3, the thiazolo[4,5-*b*]quinoxaline derivatives **2–5** and **7–9** with different substituents on positions two and three at the thiazole nucleus exhibited bioefficiency results with LC_{50} values ranging from 366.73 to 2562 mg L^{-1}. The 3-((4-methylbenzylidene) amino)thiazolo[4,5-*b*]quinoxalin-2(3*H*)-one (**3**) was the most active member on 4th larvae with the lowest LC_{50} value of 366.73 mg L^{-1} with a lower concentration value of 108.15 mg L^{-1} and an upper concentration value of 573.09 mg L^{-1}. The toxicity index revealed that compound **3** had a highly indexed 78.47%, followed by **5**, **7**, **8**, **4**, **9**, and **2** with 35.09, 25.60, 25.09, 21.58, 16.87, and 11.2%, respectively, compared to the positive control. The low toxicity slope value was recorded for 3-((3-nitrobenzylidene)amino)thiazolo[4,5-*b*] quinoxaline **5** at 0.94 ± 0.30, while *N*-(4-bromophenyl)-3-((4-chlorobenzylidene)amino)thiazolo[4,5-*b*]quinoxaline derivative **8** had the highest value at 2.09 ± 0.31.

Furthermore, the structure activity relationship (SAR) displayed that grafting an electron donating group as the methyl group to the aryl moiety of azomethane fragment (–C═N–Ar) improved the toxicological activity nearly 6.98-fold compared to the native 3-aminothiazolo[4,5-*b*]quinoxalin-2(3*H*)-one (**2**). Moreover, introducing the nitro group at the *meta* position at the 3-(benzylidene)amino fragment at C3 of thiazole increases the bio-efficiency result to be LC_{50} = 820.05 mg L^{-1}, which may be attributed to the nature of the nitro group that has an electron withdrawing nature by resonance and inductive effects. However, the presence of the chloro group at the *meta* position in the 3-(benzylidene)amino fragment showed moderate insecticidal potency, which may be attributed to the chloro atom pulling the electron (electron withdrawing natural) out to the thiazolo[4,5-*b*]quinoxaline nucleus based on the inductive effect (−I), but it could also donate electrons by resonance effect (+R), for +R > −I. In the same way, the 2,3-disubstituted thiazolo [4,5-*b*]quinoxaline-2(3*H*)-imine derivatives **7–9** showed LC_{50} values in the range of 1123.89–1705.56 mg L^{-1}, and their toxic action was assigned due to the different substituents in the two aryl groups at positions two and three on the thiazole ring. The order of toxicological activity for this series is arranged in the order of **7** (1123.89 mg L^{-1}) > **8** (1136.75 mg L^{-1}) > **9** (1705.56 mg L^{-1}). For the activity on the 4th larvae, it was found that the presence of an electron withdrawing group at position two of thiazole in thiazolo[4,5-*b*]quinoxaline-2(3*H*)-imine derivatives **7–9** decreased the activity while introducing the phenyl ring at C2 of 2-oxo-thiazole improved insecticidal activity. In addition, introducing two halogenated atoms on two aryl groups at C2 and C3 of thiazole exhibited moderate activity.

The data of the lethal time (LT_{50} = days) revealed that compound **3** killed the fourth larva in a short time at three concentrations (625, 1250, and 2500 mg L^{-1}) with LT_{50} values of 2.47, 1.96, and 1.95 days, respectively. In addition, the LC_{50} data in Table 3 and as described in Fig. 1 and 2 showed that the tested derivatives exhibited more sensitivity on the 2nd larval instar than the 4th larva. Moreover, at a low concentration of 625 mg L^{-1}, the order of lethal time by days was displayed as **3** (2.47) > **5** (5.94) > **4** (8.08) > **7** (8.72) > **8** (9.42) > **9** (10.38) > **2** (14.59), indicating that the formation of the azomethane group at C2 of thiazole revealed higher activity than 2,3-disubstituted on thiazole moiety or 3-amino-thiazole-2-one nucleus. However, the order of lethal time at a high concentration by days was **7** > **8** > **3** > **9** > **5** > **4** > **2**.

Finally, it can be concluded that the tested thiazolo[4,5-*b*] quinoxaline derivatives **2–5** and **7–9** showed good to moderate toxicological activity against the 2nd and 4th larval and these

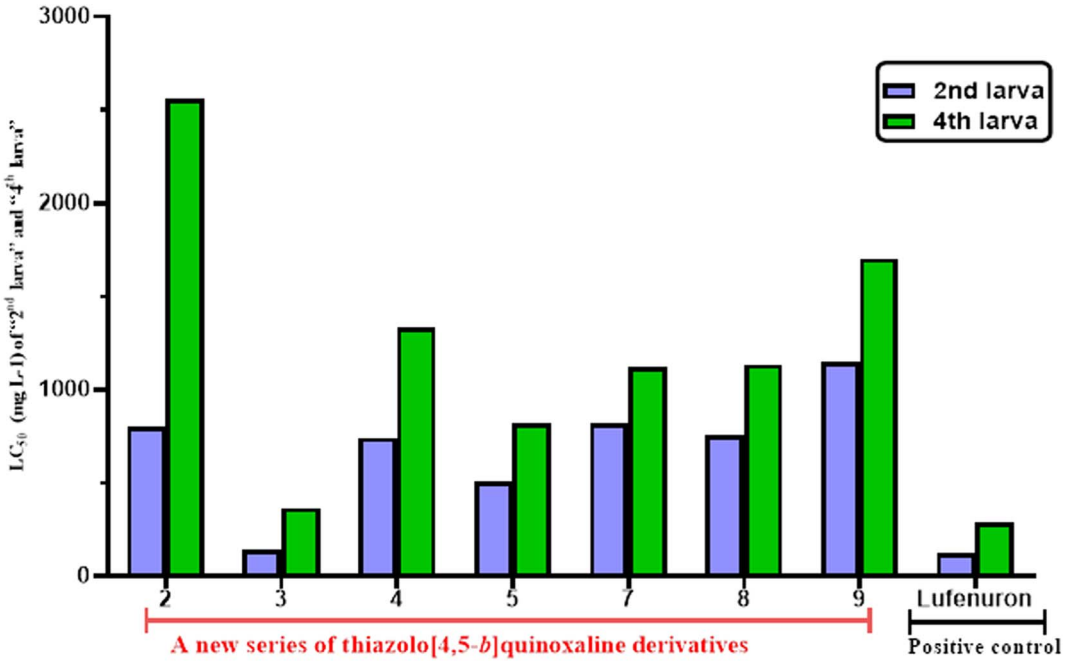

Fig. 2 LC_{50} (mg L^{-1}) values of the tested compounds against the 2nd and 4th larval instars of *S. litura*.

Open Access Article. Published on 16 January 2025. Downloaded on 2/25/2025 6:25:58 AM.
This article is licensed under a Creative Commons Attribution-NonCommercial 3.0 Unported Licence.

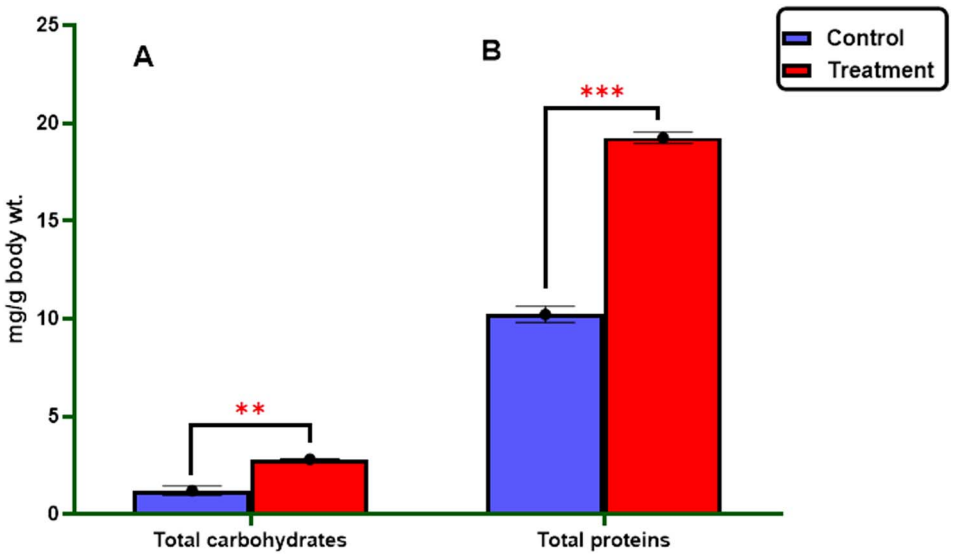

Fig. 3 Effect of the most active thiazolo[4,5-*b*]quinoxalin-2(3*H*)-one derivative **3** on the components of the 4th larval instar of *S. litura*. Error bars represent the standard error of the mean. *t* value = (A) = −6.99**, $p = 0.002$, (B) = −18.07***, $p < 0.001$.

Table 4 Total carbohydrates, total protein and enzyme activities of larvae treated with the most active thiazolo[4,5-*b*]quinoxalin-2(3*H*)-one derivative **3** compared with untreated larvae. Values are expressed as (mean ± S. E.)[a]

			Transaminases enzymes (U L^{-1})		Detoxification enzyme	
Sample	Total carbohydrate (mg per g body wt)	Total protein (mg body wt)	GPT	GOT	AlP (μg phosphate per min per mL)	AChE (μg AchBr per min per g Body wt)
Control	1.22 ± 0.23	10.22 ± 0.41	68.12 ± 0.64	58.49 ± 0.63	383.76 ± 21.54	0.64 ± 0.02
Treatment	2.82 ± 0.013	19.25 ± 0.29	62.97 ± 0.767	17.43 ± 0.04	50.22 ± 0.35	0.97 ± 0.007
t-Statistic	−6.99	−18.07	+5.17	+65.16	+15.49	−14.08
p-Value[b]	0.002	<0.001	0.007	<0.001	<0.001	0.004

[a] An increase in control (+) and treatment (−). [b] The significance level is at ≤0.05.

derivatives exhibited more sensitivity on the 2nd larval instar instead of the 4th larva.

2.2.3. Mode of action of the most effective thiazolo[4,5-*b*]quinoxalin-2(3*H*)-one derivative. The LC_{50} of the most active 3-((4-methylbenzylidene)amino)thiazolo[4,5-*b*]quinoxalin-2(3*H*)-one **3** was used for physiological, histological, and scanning electron microscopy SEM against 4th larval instar for five days.

2.2.3.1. Physiological studies

2.2.3.1.1. Total carbohydrates and proteins. As described in Fig. 3, it was found that the treatment of the most active 3-((4-methylbenzylidene)amino)thiazolo[4,5-*b*]quinoxalin-2(3*H*)-one **3** against 4th larval instar of *S. litura* revealed a significant increase in the carbohydrate content (2.82 ± 0.013 mg per g body wt) and protein levels (19.25 ± 0.29 mg per g body wt) compared to the control group (1.22 ± 0.23 and 10.22 ± 0.41 mg per g body wt), respectively (Table 4).

2.2.3.1.2. Enzyme activity. The study investigated the impact of enzymatic activity, specifically the transaminase enzymes (alanine aminotransferase (GPT) and aspartate aminotransferase (GOT)), as well as the detoxification enzymes (acetylcholinesterase AChE and alkaline phosphatase AlP), on the most potent derivatives against the *S. litura* 4th larvae after 5 days of exposure. The results are presented in Fig. 4, 5 and Table 4.

In terms of statistical analysis, the calculated t-statistic indicated a significant decrease ($P \leq 0.05$) in the levels of alanine

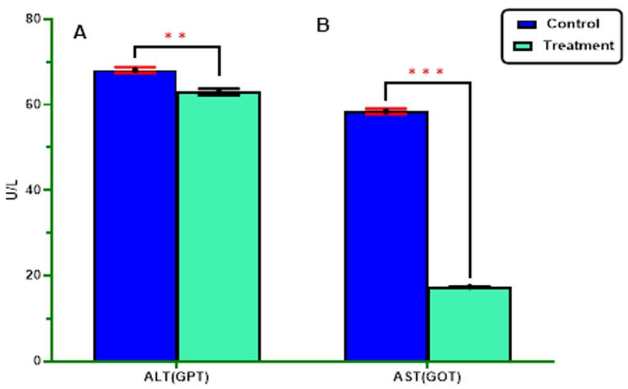

Fig. 4 ALT(GPT) and AST(GOT) activity in *S. litura* larvae after being treated with the most active thiazolo[4,5-*b*]quinoxalin-2(3*H*)-one derivative **3**. Error bars represent the standard error of the mean. *t* value = (A) +5.162** and $p = 0.007$ (B) +65.15*** and $p < 0.001$.

© 2025 The Author(s). Published by the Royal Society of Chemistry

Open Access Article. Published on 16 January 2025. Downloaded on 2/25/2025 6:25:58 AM.
This article is licensed under a Creative Commons Attribution-NonCommercial 3.0 Unported Licence.

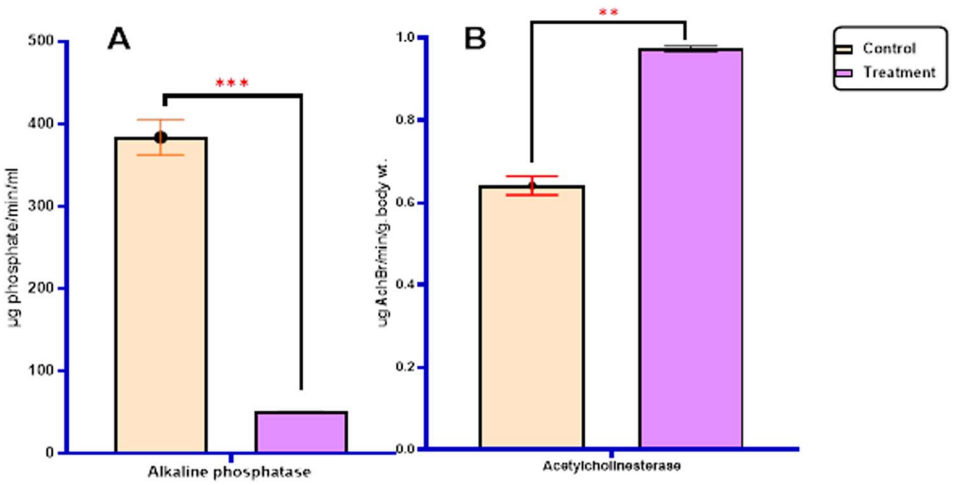

Fig. 5 (A) Alkaline phosphatase AlP. (B) Acetylcholinesterase AChE activity in *S. litura* larvae after being treated with the most active thiazolo[4,5-*b*]quinoxalin-2(3*H*)-one derivative **3**. Error bars represent the standard error of the mean. Independent samples *t* test, where *t* value (A) +15.49*** and $p < 0.001$ (B) −14.08** and $p = 0.004$.

aminotransferase (62.97 ± 0.767), aspartate aminotransferase (17.43 ± 0.04), and alkaline phosphatase (50.22 ± 0.35) compared with untreated larvae (68.12 ± 0.64), (58.49 ± 0.63), and (383.76 ± 21.54), respectively. However, the most active derivatives exhibited a significant increase in acetylcholinesterase (0.97 ± 0.009) ($P \leq 0.05$) compared with untreated larvae (0.64 ± 0.02) Fig. 4, 5 and Table 4.

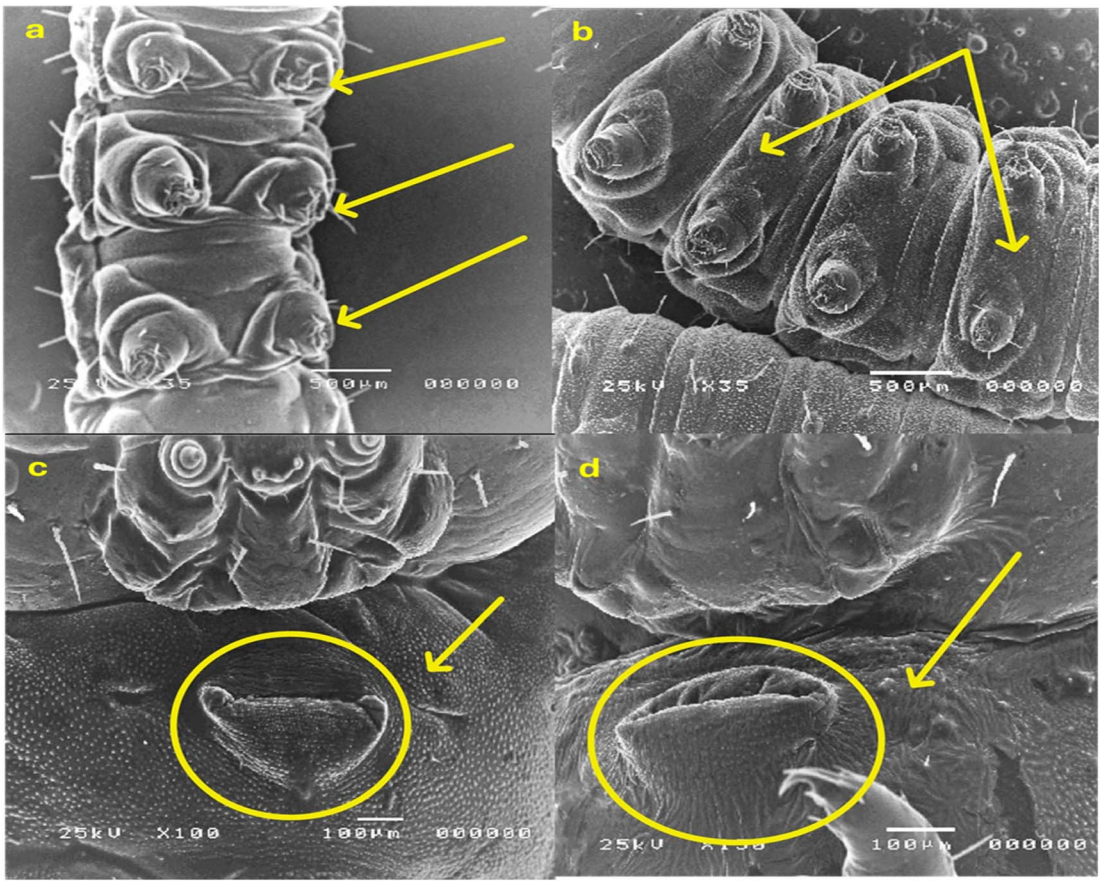

Fig. 6 SEM analysis: (a) normal larvae abdominal segments with prolegs; (b) larvae treated with LC_{50} of the most active thiazolo[4,5-*b*]quinoxalin-2(3*H*)-one derivative **3**, as shown in swelling of the space between prolegs. (c) Ventral prothorax of the normal larva; (d) larvae treated with LC_{50} of the most active thiazolo[4,5-*b*]quinoxalin-2(3*H*)-one derivative **3**, as shown in the prominent deep bulge and swelling of the ventral prothorax.

Open Access Article. Published on 16 January 2025. Downloaded on 2/25/2025 6:25:58 AM.
This article is licensed under a Creative Commons Attribution-NonCommercial 3.0 Unported Licence.

The present study is consistent with that of Assar *et al.*, who showed that all tested insecticides induced a significant inhibitory effect on alanine aminotransferase (ALT) and aspartate aminotransferase (AST) activity, except for teflubenzuron,[45] while Rashwan and his group reported that spinetoram moderately increases the activity of acetylcholinesterase.[46] Moreover, El-Mageed *et al.* demonstrated that the tested compound decreased (GOT/AST) and (GPT/ALT) activities in the hemolymph of *S. litura* 4th-instar larvae.[47] Abd El-Aswad *et al.* revealed that profenofos, chlorpyrifos, carbaryl, thiodicarb, fenpropathrin, and beta-cyfluthrin reduced ALT in the field and laboratory strains of *S. litura* in variable ways.[48] Finally, it can be concluded that our results agree with previous studies, such as Ibrahim *et al.*, who found a reduction in acetylcholinesterase from teflubenzuron,[4] and Kasmara *et al.*, who described that ALK activity was increased after the treatment of 4th and 6th instar larvae of *S. litura* with pyriproxyfen, flufenoxuron, and teflubenzuron.[49]

2.2.3.2. Morphological study using a scanning electron microscope (SEM). The morphological characteristics of *S. litura* larvae were detected through SEM analysis, as described in Fig. 6 and 7. Normal larvae treated with LC_{50} of the most active thiazolo[4,5-*b*]quinoxalin-2(3*H*)-one derivative **3** demonstrated abdominal segments with prolegs, which are differentiated in the normal (untreated) larvae. Inflammation and swelling of the space between prolegs were recorded, preventing the movement of the larvae (Fig. 6a and b). Moreover, in abnormal larvae, the deformations changed as prominent deep bulges and swelling from the ventral prothorax hindered the movement of the larva and another change (Fig. 6c and d).

Furthermore, the treated larvae exhibited changes in the diameters of their spiracles. This increase can be attributed to water loss from inside the body, leading to the dehydration of the larva compared to the untreated ones (Fig. 7a and b). Moreover, deformations and swelling were observed between the anal prolegs compared to those of the normal larva (Fig. 7c and d).

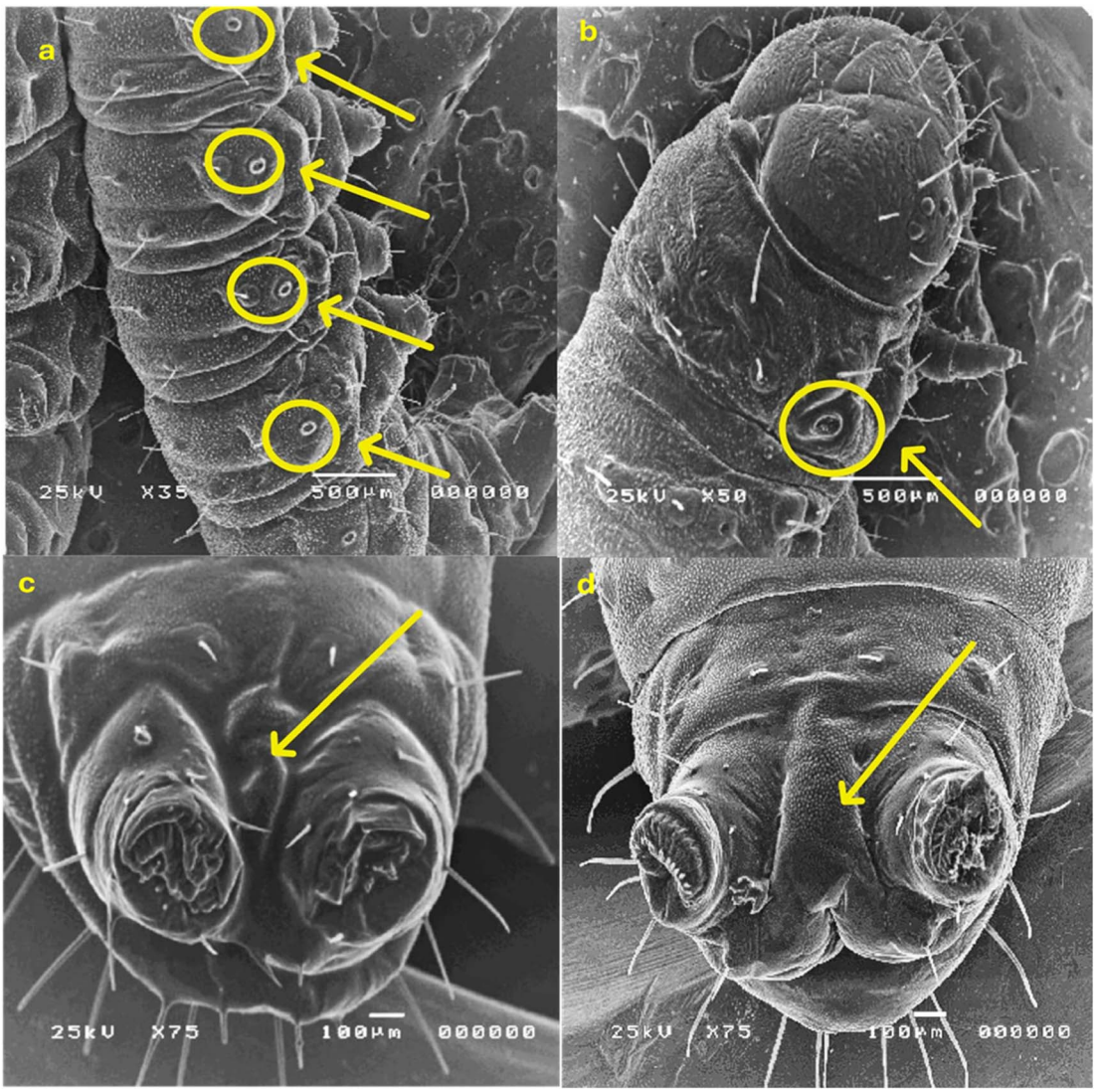

Fig. 7 SEM analysis: (a) normal diameter of spiracles; (b) larvae treated with LC_{50} of most active thiazolo[4,5-*b*]quinoxalin-2(3*H*)-one derivative **3** showed an increase in the diameter of the spiracles; (c) normal larvae showed anal prolegs; and (d) larvae treated with LC_{50} of the most active thiazolo[4,5-*b*]quinoxalin-2(3*H*)-one derivative **3**, as shown in deformations and swelling between anal prolegs.

© 2025 The Author(s). Published by the Royal Society of Chemistry

Open Access Article. Published on 16 January 2025. Downloaded on 2/25/2025 6:25:58 AM.
This article is licensed under a Creative Commons Attribution-NonCommercial 3.0 Unported Licence.

Our results agreed with previous literature observations that the treated larvae of *S. litura* were smaller than their control counterparts[50] and had several deformities in head size and body length.[51]

2.2.3.3. Histological bioassay. This study was extended to evaluate the effect of histological examination of the midgut region using LC_{50} for most active derivative **3** against the 4th larval instar of five days. One reason *S. litura* larvae die is histolysis of the gut mucosa caused by toxic effects. The longitudinal fragments of the fourth larval instar in the midgut were studied. Tall columnar cells with large nuclei in the middle of the apical area make up the typical midgut epithelium. These cells are dispersed basally with regenerative (stem) cells and apically with goblet cells. The columnar cells are towards the lumen and have a finely brushed border. As observed in Fig. 8a, several vesicles were released into an additional peritrophic area of the lumen. Moreover, many alterations can be observed in the mid intestine of the treated larvae. Several alterations become visible after five days of exposure. A few columnar cells rupture and release into the gut lumen, and cell borders vanish and split from the basement wall in the majority of the mid-gut epithelial cells. Increased vacuolation, partial cell lysis, the formation of specific vacuoles, and the removal of the peritrophic membrane are also observed. More detrimental consequences are noted, with the midgut epithelium destroyed and the gut lumen filled with dissolving cells (Fig. 8b). These outcomes are in good agreement with the results obtained by Dahi *et al.*, who observed that the epithelial cells were destroyed and removed from the basement membrane following pyridal therapy.[52] Additionally, Abdel-Aal *et al.* found that the midgut has histological consequences, such as swelling of the midgut epithelium and loss of the muscle layer's compact look. The entire peritrophic membrane was broken.[53]

The midgut plays a critical role in insect metabolic processes, as it serves as the primary site for digestion and absorption.[54] Our study's histological examination of the midgut tissues exhibited adverse effects on regenerative cells and gut epithelium. Furthermore, according to the literature, one of the key strategies for insect control involves the inhibition of gut protease activity.[55]

The epidermis is the only cellular layer in a typical integument. The other two layers, the inner foundation membrane (Fig. 9a and b) and the layer of the outer cuticle above the epidermis, are non-cellular. When the investigated chemicals were applied to the larvae of *S. litura*, significant damage to the integument was observed, resulting in total breakdown in all three layers. The molting process had various effects on the muscles, ranging from minor tissue degradation with the appearance of fissures to complete tissue loss. These findings support those of Ngegba *et al.*, who noted that the hypodermal cells displayed fissures and that the separation of the hypodermal

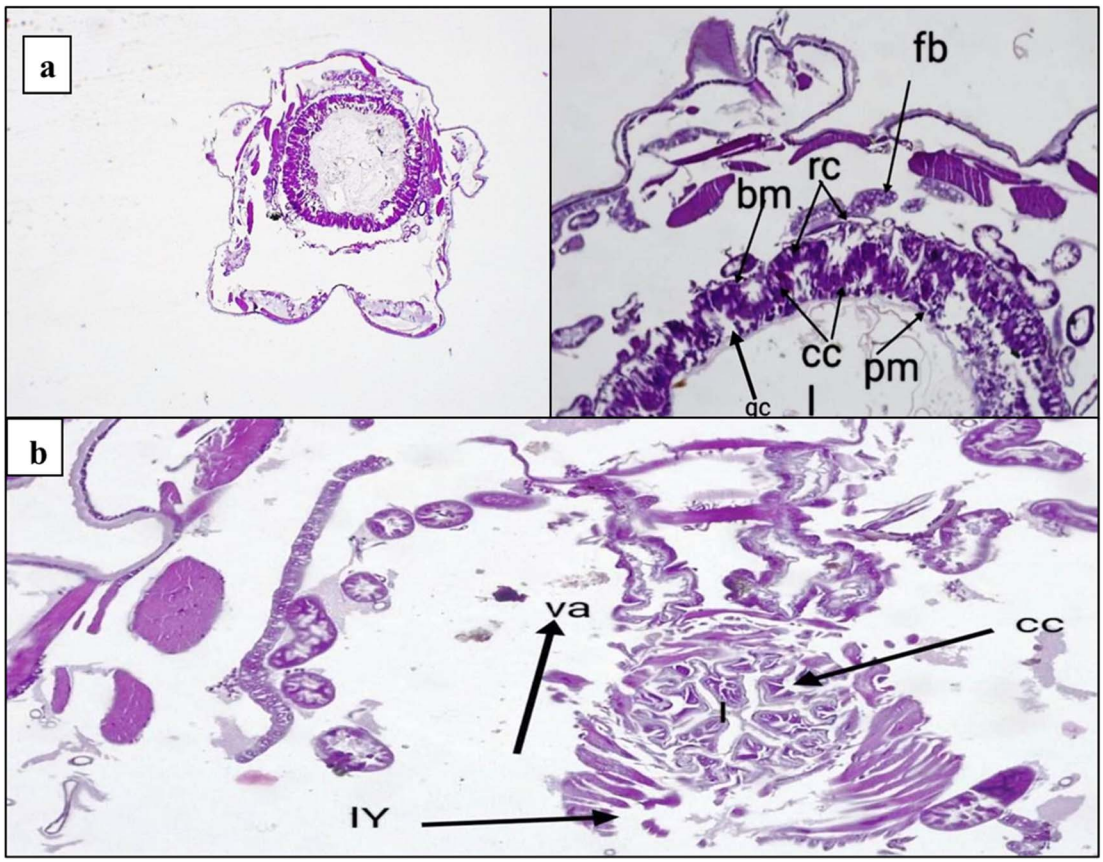

Fig. 8 (a) Anterior midgut healthy cross-section illustrating the midgut's columnar epithelial cells (cc), peritrophic membrane (pm) surrounding the gut lumen (l), basement membrane (bm) at the base of the gut epithelium, and regenerative cells (rc) beneath the fat body (fb) at the haemocoel. (b) Obliteration of the midgut epithelium after five days of exposure, with some vacuoles remaining (va) and the gut lumen filled with decayed cells (lysis of cells) (lY), along with vacuoles (va) and formation in the columnar cells (cc).

Open Access Article. Published on 16 January 2025. Downloaded on 2/25/2025 6:25:58 AM.
This article is licensed under a Creative Commons Attribution-NonCommercial 3.0 Unported Licence.

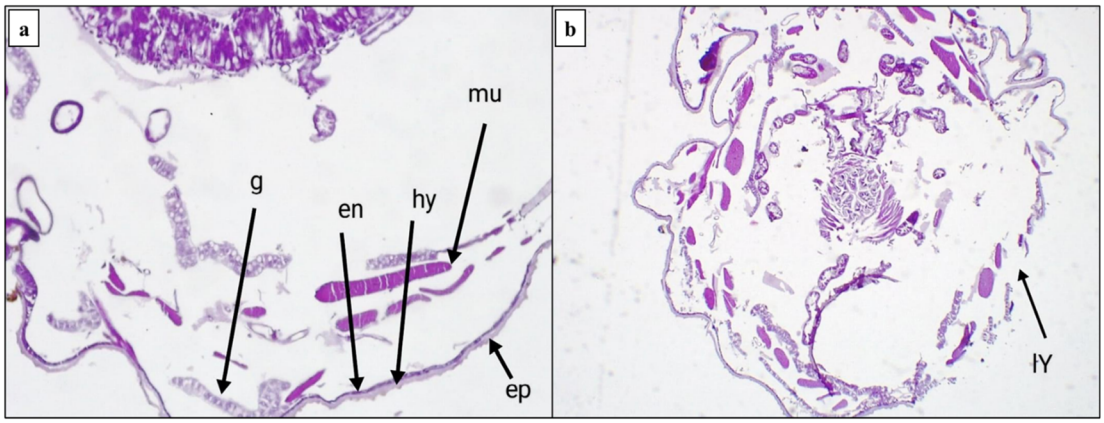

Fig. 9 (a) Normal integument cross-section, en: endocuticle ep: epicuticle g: cytoplasmic granules hy: hypodermis mu: muscles. (b) After five days of exposure, displaying destroyed cells and total integument damage (lysis of cells lY).

cells from the endocuticle was evident in the sixth larval instar of *S. litura* treated with LC_{50} of methoxyfenozide during the fourth larval instar.[56] Besides, distortion of the endocuticle was observed. This deformation revealed the breakdown of the cuticle layers, fractures in the endocuticle, and abnormal distribution of the hypodermal cells, which indicated the blocking of its creation. These elements are required for the development of the cuticle, and their absence can result in aberrant endocuticular deposition and premature molting. These outcomes are consistent with those of Hassan *et al.*[57]

2.3. *In silico* toxicity prediction

Pesticides can harm humans, pets, livestock, beneficial organisms, and the natural environment. It is important to ensure that pesticides are used safely to minimize the risk to applicators, the general public, and the environment. Therefore, we conducted an evaluation of the toxicity of the newly designed, highly potent quinoxaline compound in humans.[58] This evaluation involved the use of multiple toxicity assessments and the ProTox 3.0 web tool, as previously described.[59–61]

In terms of organ and endpoint toxicity, the prediction results revealed that compound **3** displayed inactive properties for nephrotoxicity ($P \sim 0.65$), cardiotoxicity ($P \sim 0.87$), immunotoxicity ($P \sim 0.99$), cytotoxicity ($P \sim 0.86$), clinical toxicity ($P \sim 0.52$), and nutritional toxicity ($P \sim 0.69$). Additionally, compound **3** showed an LD_{50} of nearly 1000 mg kg^{-1} with a predicted toxicity class of four. Moreover, this compound exhibited active properties for hepatotoxicity, neurotoxicity, carcinogenicity, and ecotoxicity, with low probability values ranging from 0.52 to 0.62. Furthermore, when predicting the toxicity of the most active quinoxaline derivative 3 with the ADMETlab 2.0 web tool,[62] it was found that this compound showed inactivity for skin sensitization, non-corrosiveness and non-irritation to the eyes, non-respiratory toxicity, and low toxicity for oral acute toxicity in rats.

3. Conclusion

In this study, novel thiazolo[4,5-*b*]quinoxaline derivatives **2–9** were synthesized and screened against the 2nd and 4th larval instars of the cotton leafworm *S. litura* to assess their insecticidal efficacy. The *in vivo* insecticidal efficiency (mortality%) was higher in the 2nd larval instars than in the 4th larval instars at the same concentration. These results demonstrate that the tested derivatives are toxic to *S. litura* caterpillars, affecting their feeding, respiration, and locomotion patterns. These findings could potentially be used to eliminate or control the spread of this harmful insect pest in various plant species. Because the use of conventional pesticides has led to the development of resistance in this insect, there is a continuous need for new control agents. To validate the function and behavior of the insects in relation to the response of proteins that induce disruption of essential enzymes delaying the development of *S. litura* larvae, a physiological investigation is required. The levels of acetylcholinesterase (AChE), alkaline phosphatase (AlP), alanine aminotransferase (GPT), and aspartate aminotransferase AST (GOT) were considerably affected according to the findings of the enzymatic study. A study of morphological characteristics using a scanning electron microscope (SEM) reveals that proleg-induced damage to the cuticle and head capsule hinders the mobility of larvae. Consequently, these compounds represent effective pest management strategies. These results greatly aid the practical application of these chemicals in Integrated Pest Management (IPM) programs to reduce the phenomena of resistance in this insect pest. Finally, this research proposes a methodology for scientists to explore novel quinoxaline derivatives to control the cotton leafworm *S. litura*.

4. Experimental

4.1. Chemistry

All details about the chemicals and instruments used to complete the characterization are included in the ESI† file. The starting material 2,3-dichloroquinoxaline **1** was synthesized according to previous studies with a sharp melting point M. p. = 148–150 °C.[43,44]

4.1.1. Synthesis of 3-aminothiazolo[4,5-*b*]quinoxalin-2(3*H*)-one (2). A suspension of dioxane solution containing dichloro-quinoxaline derivatives **1** (equimolar) and the

© 2025 The Author(s). Published by the Royal Society of Chemistry

Open Access Article. Published on 16 January 2025. Downloaded on 2/25/2025 6:25:58 AM. This article is licensed under a Creative Commons Attribution-NonCommercial 3.0 Unported Licence.

corresponding 2-(propan-2-ylidene)hydrazine-1-carbothioamide (equimolar) was stirred at 110 °C for 2 h (monitoring by TLC) until precipitation occurred. The suspension solution was filtered out, washed with commercial ethanol to remove the unreacted reagent, dried and recrystallized from acetonitrile to afford the pure target compound as yellow crystals with M. p.: 240–242 °C, and yield: 76%; IR (KBr, cm^{-1}): 3246, 3133 (NH_2), 3053 (sp^2-CH), 1659 (C=O), 1611 (C=N); ^1H NMR (400 MHz, DMSO-d_6) δ (ppm) 7.32 (s, NH_2, D_2O exchangeable), 7.61 (t, 1H, quinoxaline-H, J = 8.0 Hz), 7.70 (t, 1H, quinoxaline-H, J = 8.0 Hz), 7.89 (d, 2H, quinoxaline-$H_{5,8}$, J = 8.0 Hz); ^{13}C NMR (101 MHz, DMSO-d_6) δ (ppm): 125.42, 127.64, 130.29, 131.77, 135.48, 137.05 (6 Ar. Cs), 140.01(C=N), 144.59 (C=N), 155.15 (C=O); anal. calcd. for $C_9H_6N_4OS$ (218.23): C, 49.53; H, 2.77; N, 25.67; found: C, 50.15; H, 2.35; N, 25.03.

4.1.2. Synthesis of 3-((substituted-benzylidene)amino) thiazolo[4,5-*b*]quinoxalin-2(3*H*)-one (3–5)

4.1.2.1. Method I. To a solution of 1,2-dichloro-quinoxaline **2** (equimolar) and the appropriate thiosemicarbazone derivatives (equimolar), namely, 2-(2-chlorobenzylidene)hydrazine-1-carbothioamide, 2-(4-chlorobenzylidene)hydrazine-1-carbothioamide, and 2-(3-nitrobenzylidene)hydrazine-1-carbothioamide, was prepared in acetonitrile (10 mL) as the solvent. The solution mixture was stirred for 2–5 h at 100 °C (monitored by TLC). The solution was cooled to room temperature, and the precipitate was collected by filtration and crystallized from acetonitrile.

4.1.2.2. Method II. A suspension of *N*-amino thiazole derivatives **2** (equimolar) and different aldehyde derivatives, namely, *o*-chlorobenzaldehyde, *p*-chlorobenzaldehyde, and *m*-nitrobenzaldehyde, was prepared in acetonitrile (10 mL) as the solvent and catalyzed with 1 mL of acetic acid. The solution mixture was stirred under reflux conditions for 2–3 h at 100 °C (monitored by TLC). The solution was cooled to room temperature, and the precipitate was collected by filtration and crystallized from the acetonitrile.

4.1.3. 3-((4-Methylbenzylidene)amino)thiazolo[4,5-*b*]quinoxalin-2(3*H*)-one (3). Orange powder; M. p.: 163–165 °C; yield (66%); IR (KBr, cm^{-1}): 3073, 3038 (sp^2-CH), 2972 (sp^3-CH), 1654(C=O), 1602 (CH=N); ^1H NMR (400 MHz, DMSO-d_6) δ (ppm): 2.06 (s, 3H, CH_3), 7.47 (d, 2H, Ar–$H_{3,5}$, J = 6.8 Hz), 7.52 (t, 1H, quinoxaline-H, J = 7.6 Hz), 7.57 (t, 1H, quinoxaline-H, J = 8.0 Hz), 7.62 (d, 2H, Ar–$H_{2,6}$, J = 6.8 Hz), 7.68 (d, 2H, quinoxaline-$H_{5,8}$, J = 7.2 Hz), 8.45 (s, 1H, methylinic-H); ^{13}C NMR (101 MHz, DMSO-d_6) δ (ppm): 22.08 (CH_3), 120.42, 123.98, 124.29, 127.66, 128.36, 130.18, 131.20, 132.52, 135.11, 136.23 (14 Ar. Cs), 136.67 (CH=N), 151.86 (C=N), 162.32 (C=O); MS (*m*/*z*, %): 91.01 (100.00%) and 320.04 (M^+, 17.39%); anal. calcd. for $C_{17}H_{12}N_4OS$ (320.37): C, 63.73; H, 3.78; N, 17.48; found: C, 63.55; H, 3.91; N, 17.23.

4.1.4. 3-((4-Chlorobenzylidene)amino)thiazolo[4,5-*b*]quinoxalin-2(3*H*)-one (4). Brown powder; M. p.: 190–192 °C; yield (81%); IR (KBr, cm^{-1}); 3039 (sp^2-C), 1681 (C=O), 1597 (CH=N); ^1H NMR (400 MHz, DMSO-d_6) δ (ppm): 7.26 (d, 2H, Ar–$H_{3,5}$, J = 8.0 Hz), 7.74 (t, 2H, quinoxaline-H, J = 8.6 Hz), 7.80 (d, 2H, Ar–$H_{2,6}$, J = 6.8 Hz), 7.93 (d, 2H, quinoxaline-$H_{5,8}$, J = 7.6 Hz), 8.66 (s, 1H, methylinic-H); ^{13}C NMR (101 MHz, DMSO-d_6) δ (ppm): 124.72, 127.87, 128.30, 130.12, 131.34, 132.25, 136.99, 139.11, 140.63, (14 Ar. Cs), 144.99 (CH=N), 146.69 (C=N), 164.02 (C=O); MS (*m*/*z*, %): 95.44 (100.00%) and 340.49 (M^+, 62.00%); anal. calcd. for $C_{16}H_9ClN_4OS$ (340.79): C, 56.39; H, 2.66; N, 16.44; found: C, 56.43; H, 2.57; N, 16.53.

4.1.5. 3-((3-Nitrobenzylidene)amino)thiazolo[4,5-*b*]quinoxalin-2(3*H*)-one (5). Yellowish-brown powder; M. p.: 181–183 °C; yield (85%); IR (KBr, cm^{-1}): 3051 (sp^2-C), 1667 (C=O), 1615 (CH=N); ^1H NMR (400 MHz, DMSO-d_6) δ (ppm) 7.39 (d, 1H, Ar–H_5, J = 7.6 Hz), 7.69 (t, 1H, quinoxaline-H, J = 7.6 Hz), 7.78 (t, 1H, quinoxaline-H, J = 8.0 Hz), 8.16 (d, 2H, quinoxaline-$H_{5,8}$, J = 9.2 Hz), 8.28–8.31 (m, 2H, Ar–$H_{4,6}$), 8.53 (s, 1H, methylinic-H), 8.77 (s, 1H, Ar–H_5); MS (*m*/*z*, %): 113.74 (100.00%) and 351.34 (M^+, 39.83%); anal. calcd. for $C_{16}H_9N_5O_3S$ (351.34): C, 54.70; H, 2.58; N, 19.93; found: C, 55.01; H, 2.33; N, 19.15.

4.1.6. Synthesis of 3-((substituted-benzylidene)amino)-*N*-substituted-phenylthiazolo[4,5-*b*]quinoxalin-2(3*H*)-imine (7–8). A suspension of 1,2-dichloro-quinoxaline **1** (equivalent molar) and the appropriate thiosemicarbazone derivatives **6** (equimolar) was prepared in acetonitrile (10 mL) as the solvent. The solution mixture was stirred for 3–5 h at 120 °C (monitored by TLC). The solution was cooled to room temperature, and the precipitate was collected by filtration and crystallized from the acetonitrile.

4.1.7. 3-(((*E*)-Benzylidene)amino)-*N*-(2-chlorophenyl)thiazolo[4,5-*b*]quinoxalin-2(3*H*)-imine (7). Deep-orange powder; M. p.: 256–258 °C; yield (74%); IR (KBr, cm^{-1}): 3061 (sp^2-C), 1620 (CH=N); ^1H NMR (400 MHz, DMSO-d_6) δ (ppm); 7.14 (d, 2H, Ar–H, J = 8.0 Hz), 7.24 (d, 1H, Ar–H, J = 7.6 Hz), 7.48 (t, 2H, Ar–H, J = 7.8 Hz), 7.57 (t, 3H, Ar–H, J = 5.6 Hz), 7.68 (t, 2H, quinoxaline-H, J = 6.8 Hz), 7.75 (d, 1H, Ar–H, J = 8.8 Hz), 7.96 (d, 2H, quinoxaline-$H_{5,8}$, J = 8.4 Hz), 8.27 (s, 1H, methylinic-H); ^{13}C NMR (101 MHz, DMSO-d_6) δ (ppm): 120.24, 121.66, 123.39, 124.01, 124.39, 125.52, 126.10, 126.44, 127.11, 127.71, 128.29, 128.97, 130.84, 131.30, 132.34, 136.54, 137.61, 139.59 (20 Ar. Cs), 147.93 (CH=N), 154.36 (C=N); MS (*m*/*z*, %): 71.20 (100.00%) and 415.29 (M^+, 15.63%); anal. calcd. $C_{22}H_{14}ClN_5S$ (415.90): C, 63.54; H, 3.39; N, 16.84; found: C, 63.44; H, 3.43; N, 16.81.

4.1.8. 3-(((*E*)-4-Bromobenzylidene)amino)-*N*-(4-chlorophenyl)thiazolo[4,5-*b*]quinoxalin-2(3*H*)-imine (8). Red powder; M. p.: 266–268 °C; yield (71%); IR (KBr, cm^{-1}): 3040 (sp^2-C), 1639, 1599 (C=N); ^1H NMR (400 MHz, DMSO-d_6) δ (ppm): 7.09 (d, 2H, Ar–H, J = 8.4 Hz), 7.56 (d, 2H, Ar–H, J = 6.8 Hz), 7.61–7.63 (m, 2H, quinoxaline-H), 7.68 (d, 2H, Ar–H, J = 8.4 Hz), 7.83 (d, 2H, Ar–H, J = 8.4 Hz), 7.97 (d, 1H, quinoxaline-H, J = 8.4 Hz), 8.04 (d, 1H, quinoxaline-H, J = 8.4 Hz), 8.46 (s, 1H, methylinic-H); ^{13}C NMR (101 MHz, DMSO-d_6) δ (ppm): 122.76, 123.75, 124.96, 125.49, 126.88, 127.15, 127.64, 128.31, 128.59, 129.10, 130.29, 131.77, 135.93, 137.05, 138.59, 140.01 (20 Ar. Cs), 144.59 (CH=N), 155.15 (C=N); MS (*m*/*z*, %): 101.68 (100.00%) and 494.08 (M^+, 44.01%); anal. calcd. for $C_{22}H_{13}BrClN_5S$ (494.80): C, 53.40; H, 2.65; N, 14.15; found: C, 53.34; H, 2.73; N, 14.44.

4.1.9. 3-(((*E*)-4-Chlorobenzylidene)amino)-*N*-phenylthiazolo[4,5-*b*]quinoxalin-2(3*H*)-imine (9). Deep-red powder; M. p.: 277–279 °C; yield (81%); IR (KBr, cm^{-1}): 3086 (sp^2-C), 1649 (CH=N); ^1H NMR (400 MHz, DMSO-d_6) δ (ppm) 7.00–7.26 (m,

Open Access Article. Published on 16 January 2025. Downloaded on 2/25/2025 6:25:58 AM. This article is licensed under a Creative Commons Attribution-NonCommercial 3.0 Unported Licence.

4H, Ar–H), 7.48 (t, 1H, Ar–H, $J = 6.4$ Hz), 7.67 (t, 2H, Ar–H, $J = 7.2$ Hz), 7.69–7.71 (m, 2H, quinoxaline-H), 7.75 (d, 2H, quinoxaline-H, $J = 9.6$ Hz), 7.80 (d, 2H, Ar–H, $J = 6.8$ Hz), 8.45 (s, 1H, methylinic-H); ^{13}C NMR (101 MHz, DMSO-d_6) δ (ppm): 119.43, 119.85, 120.24, 120.98, 123.58, 125.10, 127.18, 127.56, 127.93, 130.33, 131.79, 133.42, 134.38, 135.98, 137.90, 140.06, 141.11 (20 Ar. Cs), 144.15 (CH=N), 153.95 (C=N); MS (*m*/*z*, %): 232.11 (100.00%) and 415.57 (M^+, 24.01%); anal. calcd. for $C_{22}H_{14}ClN_5S$ (415.90): C, 63.54; H, 3.39; N, 16.84; found: C, 63.44; H, 3.43; N, 16.81.

4.2. Insecticidal activity

4.2.1. *Spodoptera litura* colony and *in vivo* bioassay. The stock culture of *S. litura* was obtained from the Research Division of the cotton leafworm at the Plant Protection Research Institute, Agricultural Research Centre, Dokki, Giza, Egypt. The culture is known to be free from insecticide spraying and was reared under controlled laboratory conditions. These conditions included a temperature of 25 ± 5 °C, a relative humidity of 70 ± 5%, and a photoperiod of 10 h of light, followed by 14 h of darkness. The culture had been maintained under these conditions for five generations. Moreover, the *S. litura* larvae were placed in a plastic container measuring 5 × 16 × 23 cm, which was covered with muslin cloth and secured with a stretchy band. The larvae were fed fresh castor plant leaves, *Ricinus communis*.[63] The laboratory bioassay utilized 2nd and 4th instar larvae. All substances were dissolved in dimethyl sulfoxide and then diluted with distilled water at a ratio of 2 : 5, which also contained Tween 80 at a concentration of 0.1% (vol/vol). The bioassay involved dipping infested castor bean leaves in various concentrations (2500, 1250, and 625 mg L^{-1}) under the rearing conditions to assess the effects of the synthesized thiazolo[4,5-*b*]quinoxalin-2(3*H*)-one derivatives **2**, **3**, **4**, **5**, **7**, **8**, and **9** on the 2nd and 4th larval instars. The experiments were conducted with ten replicates, each consisting of 10 larvae, and the treatments were administered for 3, 5, and 7 days. As a negative control, distilled water with DMSO and Tween 80 and distilled water only were used. lufenuron, a recommended insecticide for *S. litura*, was used as a positive control.

4.2.2. Preparation of homogenate samples for biochemical analysis. Using a centrifuge, the samples were homogenized in distilled water and then centrifuged for 10 minutes at 6000 rpm at a temperature of 5 °C (using the BECKMAN GS-6R Centrifuge). After centrifugation, small aliquots (0.5 mL) of the supernatant fluid were taken and stored at −20 °C until the main components were analyzed. Each biochemical determination was replicated three times.

(1) The amount of carbohydrates was calculated according to the reported method[64] using the anthrone reagent.

(2) Total proteins were estimated by applying the method proposed by Souto *et al.*[65] using a standard of bovine serum albumin.

(3) The activities of aspartate aminotransferase (GOT) and alanine aminotransferase (ALT) were measured using DiaSys kits and the diagnostic system, in accordance with the previously reported method used by Liu *et al.* and Reitman and Frankel *et al.*[66,67] Moreover, the 4-alkaline phosphatase (AlP) activity was determined using the Powell and Smith method with some modification.[68,69] In addition, the 5-acetylcholinesterase (AChE) level was ascertained utilizing acetylcholine bromide (AChBr) as a substrate, in accordance with the method reported by Simpson *et al.* with some modifications, as described previously.[67,70]

4.2.3. Scanning electron microscopy SEM. The Applied Center for Entomopathogenic nematodes (ACE), a facility located at the Experimental Research Station at the Faculty of Agriculture, Cairo University, Giza, Egypt, is where the body of *S. litura* larvae was examined using a JEOL GM 5200 microscope. The most active thiazolo-quinoxaline derivative **3** was prepared and done in accordance with previously reported methods.[71]

4.2.4. Histological investigations of the insect midgut. The LC_{50} of thiazolo[4,5-*b*]quinoxalin-2(3*H*)-one derivative **3** on five-day-old *S. litura* larvae was used for histological examination. After being fixed for a full day, the samples were embedded in an ethanol-xylene series for dehydration. The third step was to place the sample in paraffin wax. After being cut into 4μ slices, they underwent deparaffinization, rehydration, and staining with hematoxylin and eosin for histological evaluation.[72]

4.2.5. Statistical analysis. The Statistix software (version 9.0), which is compatible with Windows, was used to conduct a statistical analysis of analysis of variance-ANOVA and independent samples *T* test of the collected data. When a significant ANOVA analysis was obtained, means were compared using Tukey's HSD test at $p \leq 0.05$. SPSS software (version 20.0) was used to determine the mortality percentage, sub-lethal concentration value (LC_{50}), and sub-lethal time (LT_{50}) with 95% confidence limits. The results were presented with regression coefficients (R^2) and regression equations ($\hat{y} = a + \beta x$), where $\hat{y}$ is the predicted value of the response variable for a given value of x (concentration), β is the slope, the amount by which y (mortality%) changes for every one-unit increase in x, and a is the intercept. The graphs were drawn with GraphPad Prism (version 9.5.1). Additionally, the toxicity index (T. I.) was determined by using the sun's equation (1950)[73] as follows:

$$\mathrm{TI} = \frac{\mathrm{LC_{50}\ of\ the\ most\ effective\ compound}}{\mathrm{LC_{50}\ of\ the\ other\ tested\ compounds}} \times 100.$$

Data availability

The data supporting this article have been included as part of the ESI† file.

Conflicts of interest

The authors declare no conflicts of interest.

Acknowledgements

The authors extend their appreciation to the Deanship of Research and Graduate Studies at King Khalid University for funding this work through the Large Research Project under grant number RGP2/91/45.

© 2025 The Author(s). Published by the Royal Society of Chemistry

Open Access Article. Published on 16 January 2025. Downloaded on 2/25/2025 6:25:58 AM. This article is licensed under a Creative Commons Attribution-NonCommercial 3.0 Unported Licence.

References

1 M. Xue, Y.-H. Pang, H.-T. Wang, Q.-L. Li and T.-X. Liu, *J. Insect Sci.*, 2010, **10**, 22.
2 S. Selvaraj, D. Adiroubane, V. Ramesh and A. L. Narayanan, *J. Biopestic.*, 2010, **3**, 43.
3 S. S. Deshmukh, C. M. Kalleshwaraswamy, B. M. Prasanna, H. G. Sannathimmappa, B. A. Kavyashree, K. N. Sharath, P. Pradeep and K. K. R. Patil, *Curr. Sci.*, 2021, 1487–1492.
4 A. M. A. Ibrahim and A. M. Ali, *J. Asia-Pac. Entomol.*, 2018, **21**, 1373–1378.
5 A. Manal and M. S. M. Zakaria, *Am. J. Biochem. Mol. Biol.*, 2013, **3**, 369–378.
6 A. Lanzoni, G. G. Bazzocchi, F. Reggiori, F. Rama, L. Sannino, S. Maini and G. Burgio, *Bull. Insectol.*, 2012, **65**, 311–318.
7 P. S. Soumia, V. Karuppaiah, V. Mahajan and M. Singh, *Natl. Acad. Sci. Lett.*, 2020, **43**, 473–476.
8 M. Saleem, D. Hussain, G. Ghouse, M. Abbas and S. W. Fisher, *Crop Prot.*, 2016, **79**, 177–184.
9 A. Thakur, P. Dhammi, H. S. Saini and S. Kaur, *J. Invertebr. Pathol.*, 2015, **127**, 38–46.
10 S. Hosseininezhad and A. Ramazani, *Arabian J. Chem.*, 2023, **16**, 105234.
11 H. F. Rizk, M. A. El-Borai, A. Ragab, S. A. Ibrahim and M. E. Sadek, *Polycyclic Aromat. Compd.*, 2023, **43**, 500–522.
12 H. Ali Mohamed, Y. A. Ammar, G. A. m. Elhagali, H. A. Eyada, D. S. Aboul-Magd and A. Ragab, *ACS Omega*, 2022, **7**, 4970–4990.
13 H. A. Mohamed, Y. A. Ammar, G. A. M. Elhagali, H. A. Eyada, D. S. Aboul-Magd and A. Ragab, *J. Mol. Struct.*, 2023, **1287**, 135671.
14 N. A. Gohar, E. A. Fayed, Y. A. Ammar, O. A. Abu Ali, A. Ragab, A. M. Mahfoz and M. S. Abusaif, *J. Enzyme Inhib. Med. Chem.*, 2024, **39**, 2367128.
15 M. S. Shah, M. M. Rahman, M. D. Islam, A. Al-Macktuf, J. U. Ahmed, H. Nishino and M. A. Haque, *J. Mol. Struct.*, 2022, **1248**, 131465.
16 M. M. Al-Sanea, M. S. Abdel-Maksoud, M. F. El-Behairy, A. Hamdi, H. Ur Rahman, D. G. T. Parambi, R. M. Elbargisy and A. A. B. Mohamed, *Bioorg. Chem.*, 2023, **139**, 106716.
17 S. A. Abdel-Aziz, E. S. Taher, P. Lan, N. A. El-Koussi, O. I. A. Salem, H. A. M. Gomaa and B. G. M. Youssif, *Arch. Pharm.*, 2022, **355**, 2200024.
18 R. Raveesha, K. Y. Kumar, M. S. Raghu, S. B. B. Prasad, A. Alsalme, P. Krishnaiah and M. K. Prashanth, *Chem. Phys. Lett.*, 2022, **791**, 139408.
19 X.-J. Peng, X.-R. Tian, S.-J. Yu, T.-T. Zhao, Q. Bian and W.-G. Zhao, *Pest Manage. Sci.*, 2023, **79**, 1977–1986.
20 G. Prashanthi, S. Kavitha, A. Velidandi and G. Mohan, *Russ. J. Org. Chem.*, 2022, **58**, 1354–1357.
21 B. Sever, M. D. Altıntop, A. Özdemir, N. Tabanca, A. S. Estep, J. J. Becnel and J. R. Bloomquist, *Open Chem.*, 2019, **17**, 288–294.
22 S. G. Parte and A. S. Kharat, *J. Environ. Public Health*, 2019, **2019**, 4807913.
23 S. Yang, J. Tang, H. Peng, C. Pu, S. Fan, C. Zhao and H. Xu, *Pest Manage. Sci.*, 2023, **79**, 5260–5269.
24 D. Nag, R. Gupta, P. Bhargav, Y. Kumar and M. S. Bisen, *Int. J. Chem. Stud.*, 2018, **6**, 1182–1186.
25 S. Sangamithra, B. Vinothkumar, N. Muthukrishnan, T. Manoharan and J. Entomol, *Zool. Stud.*, 2018, **6**, 245–249.
26 A. Ragab, D. M. Elsisi, O. A. Abu Ali, M. S. Abusaif, A. A. Askar, A. A. Farag and Y. A. Ammar, *Arabian J. Chem.*, 2022, **15**, 103497.
27 E. A. Ahmed, M. F. A. Mohamed and O. A. Omran, *RSC Adv.*, 2022, **12**, 25204–25216.
28 A. R. Al-Marhabi, H.-A. S. Abbas and Y. A. Ammar, *Molecules*, 2015, **20**, 19805–19822.
29 M. S. Abusaif, A. Ragab, E. A. Fayed, Y. A. Ammar, A. M. H. Gowifel, S. O. Hassanin, G. E. Ahmed and N. A. Gohar, *Bioorg. Chem.*, 2025, **154**, 108023.
30 N. Bouali, M. B. Hammouda, I. Ahmad, S. Ghannay, A. Thouri, A. Dbeibia, H. Patel, W. S. Hamadou, K. Hosni, M. Snoussi, M. Adnan, M. I. Hassan, E. Noumi, K. Aouadi and A. Kadri, *Molecules*, 2022, **27**, 7248.
31 A. Ragab, M. A. Salem, Y. A. Ammar, W. M. Aboulthana, M. H. Helal and M. S. Abusaif, *Drug Dev. Res.*, 2024, **85**, e22216.
32 Y. El Bakri, K. Saravanan, S. Ahmad and J. T. Mague, *J. Biomol. Struct. Dyn.*, 2023, **41**, 5277–5290.
33 M. A. Alanazi, W. A. A. Arafa, I. O. Althobaiti, H. A. Altaleb, R. B. Bakr and N. A. A. Elkanzi, *ACS Omega*, 2022, **7**, 27674–27689.
34 D. E. Burton, A. J. Lambie, D. W. J. Lane, G. T. Newbold and A. Percival, *J. Chem. Soc. C*, 1968, 1268–1273.
35 X.-H. Liu, W. Yu, L.-J. Min, D. E. Wedge, C.-X. Tan, J.-Q. Weng, H.-K. Wu, C. L. Cantrell, J. Bajsa-Hirschel, X.-W. Hua and S. O. Duke, *J. Agric. Food Chem.*, 2020, **68**, 7324–7332.
36 A. S. Rojakovick and R. B. March, *Pestic. Biochem. Physiol.*, 1976, **6**, 10–19.
37 C. O. Knowles, *Environ. Health Perspect.*, 1976, **14**, 93–102.
38 R. Ayman, M. S. Abusaif, A. M. Radwan, A. M. Elmetwally and A. Ragab, *Eur. J. Med. Chem.*, 2023, **249**, 115138.
39 R. Ayman, A. M. Radwan, A. M. Elmetwally, Y. A. Ammar and A. Ragab, *Arch. Pharm.*, 2023, **356**, e2200395.
40 A. Ragab, M. S. Abusaif, D. S. Aboul-Magd, M. M. S. Wassel, G. A. M. Elhagali and Y. A. Ammar, *Drug Dev. Res.*, 2022, 1305–1330.
41 A. S. Hassan, N. M. Morsy, W. M. Aboulthana and A. Ragab, *RSC Adv.*, 2023, **13**, 9281–9303.
42 A. Ragab, S. A. Fouad, O. A. A. Ali, E. M. Ahmed, A. M. Ali, A. A. Askar and Y. A. Ammar, *Antibiotics*, 2021, **10**, 162.
43 M. M. Abdelgalil, Y. A. Ammar, G. A. M. Elhag Ali, A. K. Ali and A. Ragab, *J. Mol. Struct.*, 2023, **1274**, 134443.
44 M. A. Ismail, M. S. Abusaif, M. S. A. El-Gaby, Y. A. Ammar and A. Ragab, *RSC Adv.*, 2023, **13**, 12589–12608.
45 A. A. Assar, M. M. Abo El-Mahasen, H. F. Dahi and H. S. Amin, *Journal of Bioscience and Applied Research*, 2016, **2**, 587–594.
46 M. H. Rashwan, *Nat. Sci.*, 2013, **11**, 40–47.

© 2025 The Author(s). Published by the Royal Society of Chemistry

Open Access Article. Published on 16 January 2025. Downloaded on 2/25/2025 6:25:58 AM. This article is licensed under a Creative Commons Attribution-NonCommercial 3.0 Unported Licence.

47 A. El-Mageed and L. R. A. Elgohary, *Pak. J. Biol. Sci.*, 2006, **9**, 713–716.
48 A. F. El-Aswad, S. A. M. Abdelgaleil and M. Nakatani, *Pest Manage. Sci.*, 2004, **60**, 199–203.
49 H. Kasmara, M. Yadav, D. A. Nurfajri, W. Hermawan and C. Panatarani, *AIP Conf. Proc.*, 2018, **1927**, 30046.
50 J. A. Leatemia and M. B. Isman, *Int. J. Trop. Insect Sci.*, 2004, **24**, 150–158.
51 R. Karimzadeh, M. J. Hejazi, F. R. Khoei and M. Moghaddam, *J. Insect Sci.*, 2007, **7**, 50.
52 H. F. Dahi, S. Aida, M. Nehad and M. F. Abd-El Aziz, *Journal of American Science*, 2011, **7**, 855–863.
53 B. Shu, J. Zhang, G. Cui, R. Sun, X. Yi and G. Zhong, *Front. Physiol.*, 2018, **9**, 137.
54 C. Ballan-Dufrançais, *Microsc. Res. Tech.*, 2002, **56**, 403–420.
55 S. Kantrao, M. A. Ravindra, S. M. D. Akbar, P. D. Kamala Jayanthi and A. Venkataraman, *J. Asia-Pac. Entomol.*, 2017, **20**, 583–589.
56 P. M. Ngegba, G. Cui, Y. Li and G. Zhong, *Pestic. Biochem. Physiol.*, 2023, **191**, 105363.
57 H. A. Hassan, *Egyptian Academic Journal of Biological Sciences. A, Entomology*, 2009, **2**, 197–209.
58 V. M. Pathak, V. K. Verma, B. S. Rawat, B. Kaur, N. Babu, A. Sharma, S. Dewali, M. Yadav, R. Kumari, S. Singh, A. Mohapatra, V. Pandey, N. Rana and J. M. Cunill, *Front. Microbiol.*, 2022, **13**, 962619.
59 H. K. Thabet, A. Ragab, M. Imran, M. Hamdy Helal, S. Ibrahim Alaqel, A. Alshehri, A. Ash Mohd, S. S. Alshammari, Y. A. Ammar and M. S. Abusaif, *RSC Adv.*, 2024, **14**, 15691–15705.
60 H. K. Thabet, M. S. Abusaif, M. Imran, M. H. Helal, S. I. Alaqel, A. Alshehri, A. A. Mohd, Y. A. Ammar and A. Ragab, *Comput. Biol. Chem.*, 2024, **111**, 108097.
61 H. Khamees Thabet, A. Ragab, M. Imran, M. H. Helal, S. Ibrahim Alaqel, A. Alshehri, A. Ash Mohd, M. Rakan Alshammari, M. S. Abusaif and Y. A. Ammar, *Eur. J. Med. Chem.*, 2024, **275**, 116589.
62 A. Ragab, S. A. Ibrahim, D. S. Aboul-Magd and M. H. Baren, *RSC Adv.*, 2023, **13**, 34756–34771.
63 M. Zhang, Y. Demeshko, R. Dumbur, T. Iven, I. Feussner, G. Lebedov, M. Ganim, R. Barg and G. Ben-Hayyim, *J. Plant Growth Regul.*, 2019, **38**, 723–738.
64 Y.-P. Gao, M. Luo, X.-Y. Wang, X. Z. He, W. Lu and X.-L. Zheng, *Insects*, 2022, **13**, 914.
65 A. L. Souto, M. Sylvestre, E. D. Tölke, J. F. Tavares, J. M. Barbosa-Filho and G. Cebrián-Torrejón, *Molecules*, 2021, **26**, 4835.
66 S. Reitman and S. Frankel, *Am. J. Clin. Pathol.*, 1957, **28**, 56–63.
67 X.-Y. Liu, S.-S. Wang, F. Zhong, M. Zhou, X.-Y. Jiang, Y.-S. Cheng, Y.-H. Dan, G. Hu, C. Li, B. Tang and Y. Wu, *Front. Physiol.*, 2022, **13**, 1034926.
68 M. E. A. Powell and M. J. H. Smith, *J. Clin. Pathol.*, 1954, **7**, 245–248.
69 K. Hamadah, K. Ghoneim, M. Tanani, A. Basiouny and H. Waheeb, *Int. J. Adv. Res.*, 2016, **4**, 611–624.
70 D. R. Simpson, D. L. Bull and D. A. Lindquist, *Ann. Entomol. Soc. Am.*, 1964, **57**, 367–371.
71 A. Ragab, D. M. Elsisi, E. M. Elqady, E. EL-Said, M. A. Salem, Y. A. Ammar and M. S. Abusaif, *Pestic. Biochem. Physiol.*, 2024, **202**, 105943.
72 H. A. Borei, M. F. M. El-Samahy, O. A. Galal and A. F. Thabet, *Global Journal of Agriculture and Food Safety Sciences*, 2014, **1**, 161–168.
73 Y.-P. Sun, *J. Econ. Entomol.*, 1950, **43**, 45–53.

© 2025 The Author(s). Published by the Royal Society of Chemistry